under the following conditions: 48 °C for 30 min, 95 °C for 10 min, 50 cycles of 95 °C for 15 s, and 60 °C for 1 min. Standard curves were constructed on a 1:5 serial dilution of the RNA template. The results were normalized to GAPDH mRNA levels.

Determination of Protein Stability—HuH-7 cells were infected with HCV JFH-1 at a m.o.i. of 2. Six hours after infection, the cells were either treated with KIF or transfected with EDEM1 siRNA. Forty hours later, culture medium was replaced with 100 μg/ml cycloheximide (CHX). Cells, including floating cells, were harvested at different time points after CHX addition, and immunoblotting was performed to determine the amount of HCV E2.

Plasmid Transfection and Immunoprecipitation—HuH-7 or 293T cells were seeded in 6-well cell culture plates at 3×10^5 cells/well and cultured overnight. Plasmid DNA was transfected into cells using TranIT-LT1 transfection reagent (Mirus, Madison, WI). Cells were harvested at 48 h after transfection, washed once with 1 ml of PBS, and lysed in 200 μl of lysis buffer (20 mM Tris-HCl, pH 7.4, 135 mM NaCl, 1% Triton X-100, and 10% glycerol supplemented with 50 mM NaF, 5 mM Na_3VO_4, and protease inhibitor mixture tablets (Roche Diagnostics). Cell lysates were sonicated at 4 °C for 10 min, incubated for 30 min at 4 °C, and centrifuged at 14,000 × g for 5 min at 4 °C. After preclearing for 2 h, the supernatants were immunoprecipitated overnight by rotating with 1.5 μl of anti-HA monoclonal antibody (16B12) or anti-HCV E2 monoclonal antibody (clone 8D10-3) at 4 °C. The immunocomplexes were then captured on protein G-agarose beads (Invitrogen) by rotation-incubation at 4 °C for 3 h. Beads were subsequently precipitated by centrifugation at 800 × g for 1 min and washed five times with lysis buffer. Finally, proteins bound to the beads were boiled in 40 μl of SDS sample buffer and subjected to SDS-PAGE.

Western Blotting—Proteins resolved by SDS-PAGE were transferred onto PVDF membranes (Immobilon; Millipore). After blocking in 2% skim milk, the membranes were probed with primary antibodies followed by exposure to peroxidase-conjugated secondary antibodies and visualization with an ECL Plus Western blotting detection system (GE Healthcare). The intensity of the bands was measured using a computerized imaging system (ImageJ software; National Institutes of Health).

Small Interfering RNA (siRNA) Transfection—HuH-7 cells were transfected with duplex siRNAs at a final concentration of 10 nM using Lipofectamine RNAiMAX (Invitrogen). Three siRNAs for each gene were examined for knock-down efficiency and cytotoxic effects. The siRNA with best performance was selected for further experiments. Target sequences of the siRNAs which exhibited the best knock-down efficiencies were as follows: EDEM1 (sense) 5′-CAUAUCCUCGGGUGAAU-CUtt-3′, EDEM2 (sense) 5′-GAAUGUCUCAGAAUUC-CAAtt-3′, EDEM3 (sense) 5′-CAUGAGACUACAAAUC-UUAtt-3′, IRE1 (sense) 5′-GGACGUGAGCGACAGAAUAtt-3′. 5′-GGUGUCCUUACCAUACUAAtt-3′ served as a negative control. The lowercase letters denote overhanging deoxyribonucleotides.

Quantification of HCV Core and RNA—HCV core was quantified using an enzyme immunoassay (Ortho HCV antigen ELISA kit; Ortho Clinical Diagnostics, Tokyo, Japan). HCV RNA was quantified as described (17).

Statistical Analysis—Student's t test was employed to calculate the statistical significance of the results. $p < 0.05$ was considered significant.

RESULTS

HCV Infection Induces XBP1 mRNA Splicing and EDEM Expression—XBP1 plays a key role in activating the ERAD pathway, which mediates unfolded protein response in the ER. Under conditions of ER stress, XBP1 mRNA is processed by unconventional splicing and translated into functional XBP1, which in turn mediates transcriptional up-regulation of a variety of ER stress-dependent genes. The resultant activation of downstream pathways boosts the efficiency of ERAD, which coincides with elevated transcription of EDEMs. To validate our method for detecting activation of the ERAD pathway, we exposed HuH-7.5.1 cells to TM, which is a typical ER stress inducer, and performed an assay to quantify spliced XBP1 mRNA, as described under "Experimental Procedures," at different time points after treatment. The spliced form of XBP1 mRNA started accumulating within these cells as early as 2 h after exposure to TM (Fig. 1*A*), and levels remained elevated until at least 12 h after treatment. Quantitative RT-PCR showed that mRNA levels of EDEM1, EDEM2, and EDEM3 were elevated in TM-treated cells whereas ER ManI, which is not an ER stress-responsive gene, did not show any up-regulation (Fig. 1*B*). To examine involvement of the ERAD pathway in the HCV life cycle, we infected HuH-7.5.1 cells with JFH-1 at m.o.i. of 5 and analyzed XBP1 mRNA splicing and EDEM up-regulation. Upon infection, the fragment corresponding to spliced XBP1 mRNA, was detectable 8 h after infection, and the difference in splicing between mock- and HCV-infected cells became more pronounced at 48 h after infection and then persisted (Fig. 1*C*). Increased levels of XBP1 mRNA splicing were dependent on the m.o.i. (supplemental Fig. 1*A*), suggesting that expression of active XBP1 was induced by HCV infection. A small amount of spliced XBP1 was detected in mock-infected cells, presumably because of some intrinsic stress. A 3.1-fold increase in the level of EDEM1 mRNA was observed at 3–4 days after infection ($p < 0.05$). Increases in EDEM2 and EDEM3 mRNA levels were moderate and reached ~1.5-fold, whereas ER ManI mRNA exhibited no change after infection (Fig. 1*D*). Expression of EDEMs, particularly EDEM1, was up-regulated in accordance with HCV infection titers (supplemental Fig. 1*B*). Knocking down the IRE1 gene (Fig. 1*E*) effectively reversed the accumulation of spliced XBP1, as well as the transcriptional up-regulation of EDEM1 (Fig. 1*F*), thus confirming that HCV infection induces ERAD through the IRE1-XBP1 pathway.

To enable a comprehensive investigation of the transcriptional changes that occur, up- and down-regulation of the transcriptome was examined in HCV-infected cells and in TM-treated cells. The results were compared with those of mock-transfected cells at each time point. A range of genes involved in ER stress was found to be regulated in HCV-infected and in TM-treated cells (Fig. 2*A*). EDEM1 was signifi-
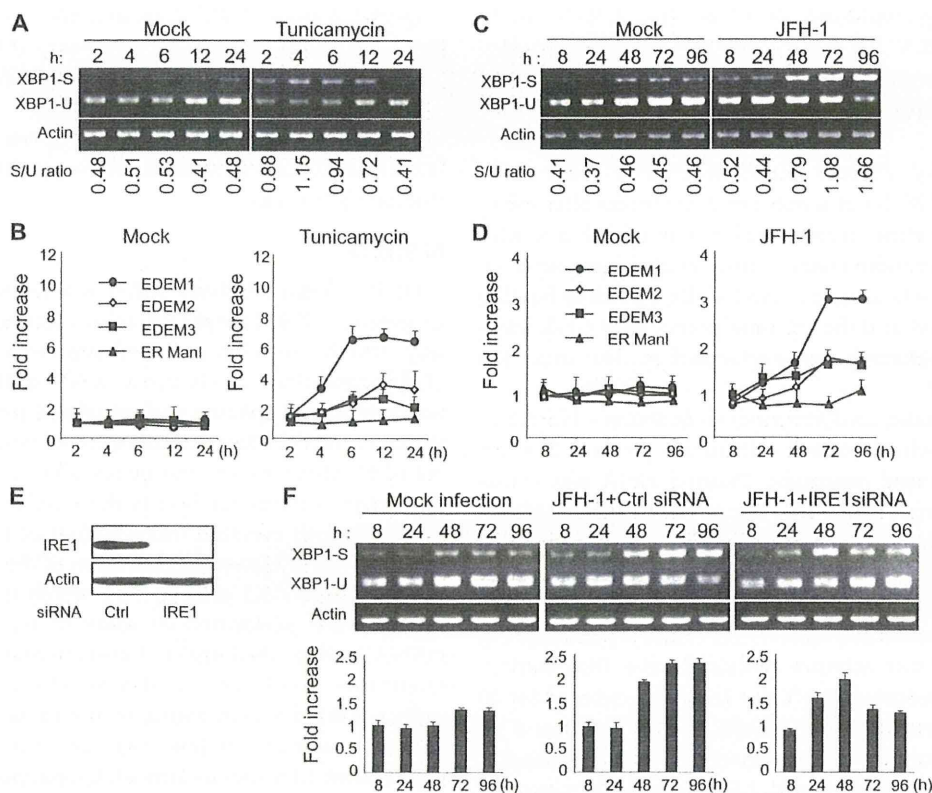
– 361 –

FIGURE 1. **Splicing of XBP1 mRNA and induction of ERAD gene expression in HCV JFH-1-infected cells.** *A*, splicing of XBP1 mRNA analyzed in mock- and TM (5 μg/ml)-treated HuH-7.5.1 cells at different time points after treatment. The *upper* and *lower bands* represent spliced and unspliced RNA, respectively. The *numbers* at the *bottom* of the *panel* indicate the density ratios of bands corresponding to spliced and unspliced XBP1. *B*, graphs showing the -fold induction of EDEM1, EDEM2, EDEM3, and ER ManI mRNA in HuH-7.5.1 cells treated or untreated with TM. Data are normalized to GAPDH expression levels. The mean ± S.D. (*error bars*) of three independent experiments are shown. *C*, splicing of XBP1 mRNA analyzed in mock- and HCV JFH-1-infected HuH-7.5.1 cells (m.o.i. 5) at different time points after infection. *Numbers* at the *bottom* of the *panel* indicate the density ratios of bands corresponding to spliced and unspliced XBP1. *D*, real-time PCR analysis of EDEM1, EDEM2, EDEM3, and ER ManI mRNA induction in mock- and HCV-infected cells. Data are normalized to GAPDH expression. The mean ± S.D. of three independent experiments are shown. Note that a reduction in the level of GAPDH mRNA within infected cells was not observed until 96 h after infection when a slight decrease was observed. This led us to use GAPDH as a housekeeping gene in our experiments. *E*, Western blotting of IRE1 in cells transfected with mock or gene-specific siRNA of IRE1. *F*, splicing of XBP1 mRNA and induction of EDEM1 in HCV-infected cells after knocking down of the IRE1 gene. HuH-7.5.1 cells infected with JFH-1 at a m.o.i. of 5 were transfected with mock (*center*) or IRE1-specific siRNA (*right*) 48 h after infection, after which splicing of XBP1 (*upper*) and transcriptional up-regulation of EDEM1 (*lower*) were examined at the indicated time points after infection. The mean ± S.D. of two independent experiments are shown.

cantly up-regulated upon HCV infection, whereas expression levels of EDEM2 and EDEM3 remained unchanged. Although transcriptional changes caused by HCV infection in many of the genes listed are analogous to those that occur in cells treated with TM, up-regulation of two ER chaperone proteins, GRP78 and GRP94, was induced by TM treatment but not by HCV infection. This differential induction was confirmed by a reporter assay for GRP78 promoter and GRP94 promoter activities (Fig. 2*B*). These results are in agreement with a previously described finding that GRP78 and GRP94 are not responsive to HCV infection in hepatoma cells (18). It remains likely that HCV infection interferes with transcriptional activation of some ER chaperone proteins; however, the mechanism by which this occurs remains to be elucidated.

EDEMs Cause Ubiquitylation of HCV Glycoproteins and Enhance Their Degradation—Because EDEMs have been reported to enhance proteasomal degradation of ERAD substrates through direct binding, we investigated the interaction of EDEMs with HCV glycoproteins in 293T cells by co-transfecting the expression plasmids for E1dTM or E2dTM together with plasmids carrying either EDEM or ER ManI genes. Immu-

noprecipitation and immunoblotting demonstrated that each EDEM, but not ER ManI, was capable of interacting with E2 (Fig. 3*A*) and E1 (supplemental Fig. S2). HCV glycoproteins displayed enhanced mobility when co-expressed with EDEM1, EDEM3, or ER ManI, which could be due to the mannosidase activity of these proteins, which is lacking in EDEM2 (6). HCV primarily replicates in hepatocytes so we examined the interaction of EDEMs with E2dTM in HuH-7 cells as well, which yielded similar results (data not shown). E2dTM lacks the transmembrane domain, which could affect its folding and ER retention and thus modulate the ability of this protein to interact with EDEMs and ER ManI. Second, E1 and E2 glycoproteins assemble as noncovalent heterodimers to make functional complexes, which may alter the interaction of these proteins with EDEMs. To address these issues, we co-transfected HuH-7 cells with plasmids carrying full-length E1E2 glycoproteins together with plasmids carrying either EDEMs or ER ManI. Similar phenotypes were produced following transfection full-length E1E2 proteins (supplemental Fig. S3*A*), demonstrating that functional complexes of HCV glycoproteins bind with EDEMs. Recently, we have reported on the development of a
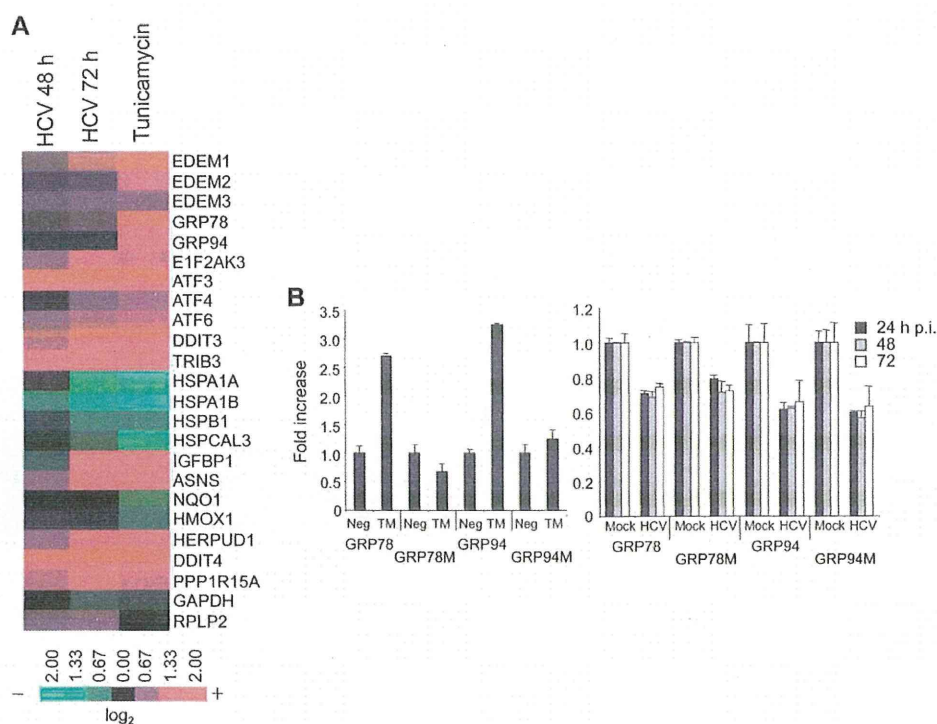
– 362 –

FIGURE 2. **Comprehensive analysis of ERAD gene expression in JFH-1-infected HuH-7.5.1 cells.** *A*, HuH-7.5.1 cells treated with TM (5 μg/ml) for 12 h or infected with JFH-1 for 48 and 72 h were subjected to microarray analysis, along with their negative controls. Expression of ER stress genes is shown as a heat map. *Red* and *green* indicate up- and down-regulation, respectively. Information on each gene shown is indicated on the 3D-Gene web site. *B*, GRP78 and GRP94 induction in TM-treated (*left*) and HCV-infected cells (*right*). GRP78M and GRP94M represent the defective promoters. The mean ± S.D. (*error bars*) of three independent experiments are shown.

packaging system of HCV subgenomic replicon sequences through the provision of viral core NS2 proteins in *trans* (19). Transcomplementation with core NS2 proteins resulted in successful packaging of the viral sequences; therefore, plasmids carrying these proteins are a valid construct by which to examine the interaction of envelope proteins with ERAD machinery. Thus, we performed an immunoprecipitation assay of HuH-7 cells co-transfected with core NS2 and EDEMs. In agreement with our previous results, EDEMs, but not ER ManI, were observed to bind to HCV E2 protein (supplemental Fig. S3B). To examine the functional importance of this interaction, we analyzed the ubiquitylation of HCV E2 protein in cells co-transfected with HCV E2 and EDEM proteins. An immunoprecipitation assay revealed that overexpression of EDEM1 and EDEM3, but not of EDEM2 and ER ManI, dramatically increased the ubiquitylation of HCV glycoprotein (Fig. 3B). In mammals, the ER membrane ubiquitin-ligase complex involved in the dislocation of ERAD substrates, and their ubiquitylation contains the ER membrane adaptor SEL1L. It has recently been shown that SEL1L interacts with EDEM1 in cells and functions as a cargo receptor for ERAD substrates (20); however, it is unknown whether SEL1L interacts with other EDEMs. We therefore assessed whether SEL1L interacts with EDEM1, EDEM2, EDEM3, and ER ManI in cells (Fig. 3C). Interestingly, endogenous SEL1L co-precipitated with EDEM1 and EDEM3, whereas little to no interaction was observed with EDEM2 and ER ManI. Collectively, it is likely that, although all EDEMs can recognize HCV E1 and E2, EDEM1 and EDEM3 are involved in the ubiquitylation of HCV glycoproteins by deliver-

ing them to SEL1L-containing ubiquitin-ligase complexes. To investigate further the role of EDEMs in quality control of HCV glycoproteins, we measured the steady-state level of HCV E2 protein after EDEM knockdown. Transfection of HCV-infected cells with siRNAs against EDEM1, EDEM2, or EDEM3 caused a 60–80% reduction in mRNA levels of the respective genes (Fig. 3D) with no cytotoxic effects observed (data not shown). Immunoblotting showed a considerable increase in the steady-state level of viral E2 in EDEM1 siRNA-treated cells (Fig. 3D). We subsequently examined the turnover of E2 in cells with and without EDEM1 knockdown. In CHX half-life experiments, E2 protein was moderately unstable in control-infected cells, presumably via proteasomal degradation (Fig. 3E). Treatment with MG132, a proteasome inhibitor, blocked its destabilization (data not shown). In contrast, E2 was completely stable in EDEM1-knockdown cells during the chase period of time tested (Fig. 3E). Together, these results strongly suggest that EDEM1 and EDEM3, particularly EDEM1, are involved in the post-translational control of HCV glycoproteins.

Involvement of EDEM1 in the Production of Infectious HCV—Given the involvement of EDEMs in the turnover of HCV glycoproteins, we investigated whether EDEMs affect the replication and production of infectious virus particles. EDEMs were knocked down in HCV-infected HuH-7 cells by siRNA transfection, and the production of infectious particles was then monitored by measuring the extracellular infectivity titer. Knocking down of EDEM1 and EDEM3 in the infected cells resulted in ~3.1-fold ($p < 0.05$) and ~2.3-fold increases in virus production, respectively, compared with control cells. No effect
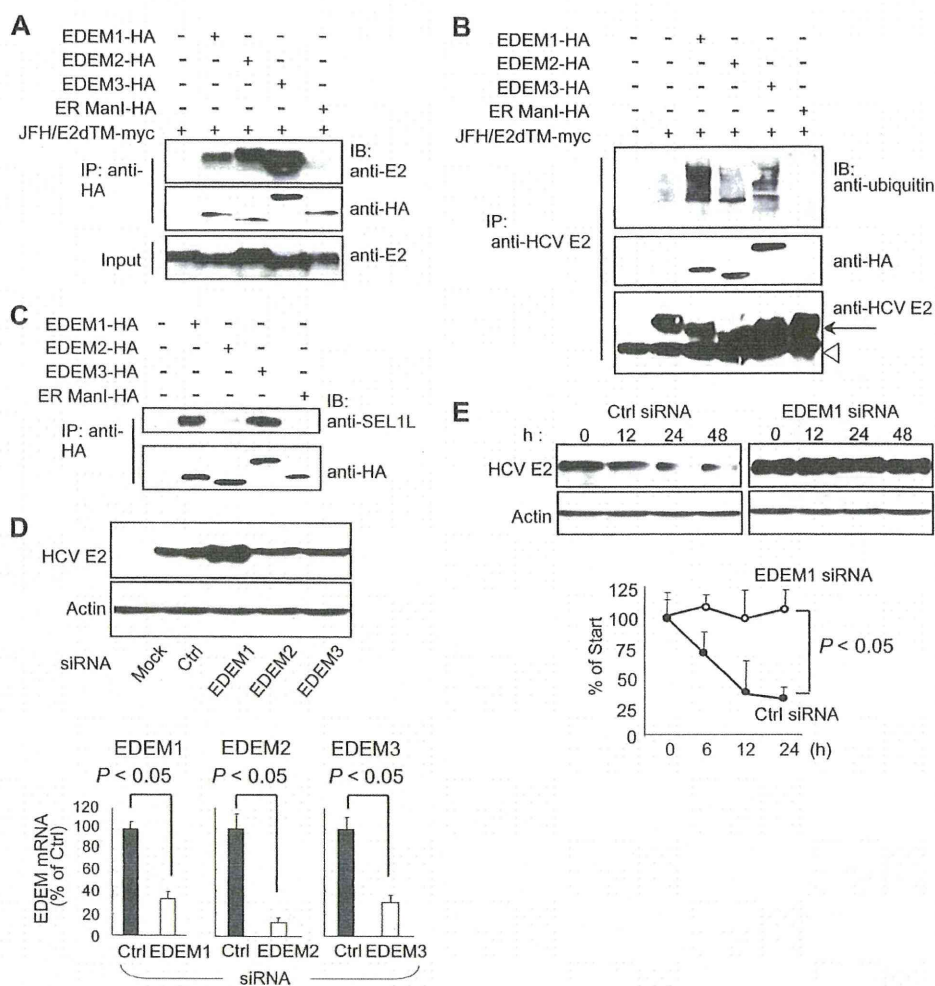
– 363 –

FIGURE 3. **EDEMs are involved in the degradation of HCV glycoproteins.** *A*, binding of EDEMs and ER ManI with HCV E2. 293T cells were seeded in 6-well plates at a density of 3×10^5 cells/well. After overnight incubation, cells were co-transfected with plasmids carrying HCV E2-myc (1 μg) and EDEM1-HA, EDEM2-HA, EDEM3-HA, or ER ManI-HA proteins (1 μg each). Forty-eight hours later, cells were harvested, immunoprecipitated (*IP*) with anti-HA antibodies, and Western blotting (*IB*) was performed with the indicated antibodies. *B*, ubiquitylation of HCV E2 protein in cells co-transfected with HCV E2 and EDEM plasmids. 293T cells were seeded in 6-well plates at a density of 3×10^5 cells/well. Twenty-four hours later, the cells were co-transfected with plasmids carrying HCV E2-myc (1 μg) and EDEM1-HA, EDEM2-HA, EDEM3-HA, or ER ManI-HA genes (1 μg each). Forty-eight hours later, the cells were harvested and immunoprecipitated with anti-E2 antibodies, and Western blotting was performed with the indicated antibodies. *Arrow*, HCV E2; *open arrowhead*, immunoglobulin heavy chain. *C*, binding of EDEMs and ER ManI with endogenous SEL1L in cells. *D*, steady-state level of HCV E2 in HCV-infected HuH-7 cells after EDEM knockdown (*upper*). The knockdown efficiencies of the respective siRNAs are shown in the *lower panel*. Values are normalized to GAPDH expression levels, and normalized values in negative control cells have been arbitrarily set at 100%. *E*, stability of HCV E2 protein in EDEM1 knockdown cells. HCV-infected HuH-7 cells were transfected with control or EDEM1 siRNA. Forty hours later, the cells were exposed to CHX (100 μg/ml) for 0, 12, 24, and 48 h, followed by immunoblotting. Specific signals were quantified by densitometry, and the percent of HCV E2 remaining was compared with initial levels. The mean $\pm$ S.D. (*error bars*) of two independent experiments are shown.

on virus production was observed following EDEM2 gene silencing (Fig. 4*A*). On the other hand, no significant differences were observed with regard to intracellular HCV core protein levels among mock- and EDEM siRNA-transfected cells (Fig. 4*B*), which indicates that replication of the viral genome is not affected by EDEM proteins. To examine further whether this effect on virus production was due to turnover of HCV envelope proteins, we performed loss-of-EDEM-function experiments in HuH-7 cells carrying HCV subgenomic replicons. Because the replicons do not require envelope proteins, they should be insensitive to the expression levels of genes involved in the ERAD pathway. As expected, siRNA-mediated knockdown of EDEMs resulted in little to no change in genome replication (supplemental Fig. S4*A*). To investigate further the participation of EDEMs in the

HCV life cycle, HCV-infected cells were examined 48 h after transfection with an expression plasmid for either EDEM1, EDEM2, or EDEM3. As expected, exogenous expression of EDEM1 in the infected cells led to a 2.4-fold decrease in virus production compared with mock-transfected cells ($p < 0.05$) (Fig. 4*C*). A moderate decrease of 1.7-fold was observed in the cells overexpressing EDEM3 protein. Ectopic expression of EDEMs and ER ManI did not cause any change in intracellular HCV core protein levels (Fig. 4*D*). Similarly, little or no change was observed in genome replication when plasmids carrying EDEMs were introduced into HCV subgenomic replicon cells (supplemental Fig. S4*B*). These results indicate that EDEM1 and EDEM3, particularly EDEM1, regulate virus production, possibly through post-translational control of HCV glycoproteins.
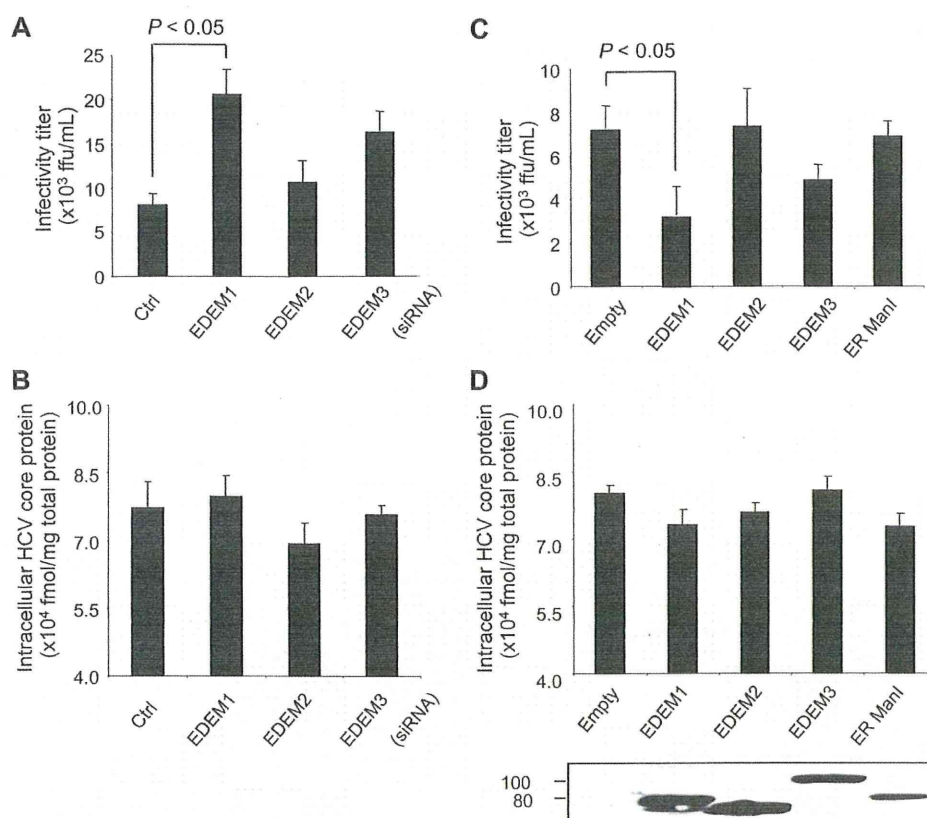
FIGURE 4. **Role of EDEMs in HCV replication and production of infectious virus particles.** *A*, HCV production in HuH-7 cells transfected with EDEM siRNAs. Cells were infected with JFH-1 at a m.o.i. of 1. Twenty-four hours later, the cells were transfected with the indicated siRNAs at a final concentration of 10 nM. The culture medium was harvested 48 h later and was used to infect naïve HuH-7.5.1 cells seeded in a 96-well plate. Immunostaining using anti-HCV core antibodies was performed at 72 h after infection, and focus-forming units were counted. *B*, siRNA-transfected and HCV-infected cells described in *A* harvested at 48 h after infection. Intracellular HCV core protein was measured. The values were normalized to total protein in the cell lysate samples. *C*, HCV production in HuH-7 cells transfected with plasmids carrying EDEM1-HA, EDEM2-HA, EDEM3-HA, or ER ManI-HA genes. *D*, intracellular HCV core protein within the cells described in *C*. Expression levels of the EDEMs and ER ManI were determined by anti-HA immunoblotting. The mean ± S.D. (*error bars*) of three independent experiments are shown in all of the *panels*.

Chemical Inhibition of the ERAD Pathway Increases HCV Production—KIF, a potent inhibitor of ER mannosidase, is reported to inhibit the ERAD pathway. When HCV-infected cells were treated with KIF, virus production increased in the culture medium in a dose-dependent manner (Fig. 5*A*, *left*), and the steady-state level of E2 in the cells increased accordingly (Fig. 5*A*, *right*). No change was observed in intracellular HCV core protein levels after KIF treatment (Fig. 5*A*, *center*). Kinetic analyses showed that E2 was stabilized dramatically in KIF-treated cells (Fig. 5*B*), whereas the fate of HCV core protein, a nonglycoprotein, was not affected by KIF treatment (supplemental Fig. S5). No effect on virus replication was observed when the cells harboring JFH-1 subgenomic replicons were treated with KIF (data not shown).

On the basis of these findings, one may hypothesize that KIF contributes to the stabilization of HCV glycoprotein(s) by interfering with the interaction between (i) EDEMs and viral proteins, or (ii) EDEMs and SEL1L. To address this, HCV E2 was co-expressed in 293T cells with EDEM1, EDEM2, EDEM3, or ER ManI in the presence or absence of KIF, followed by immunoprecipitation (Fig. 5*C*). E2 was shown to interact with EDEM1, EDEM2, and EDEM3, analogous to the data shown in Fig. 3*A*, and KIF did not block the interactions. Decreased electrophoretic mobility of E2 was detected in KIF-treated cells,

possibly due to a change in glycan composition caused by inhibition of mannosidase activity. These findings led us to investigate whether the glycans on HCV glycoproteins are required for binding to EDEMs. We generated E1 and E2 mutants by replacing their N-glycosylation sites with glutamine residues and analyzed their interaction with EDEMs. Removal of the glycans did not inhibit the binding of E1 and E2 proteins to EDEM, demonstrating that N-glycans on the surface of viral proteins are not indispensible for an interaction between EDEMs and HCV glycoproteins to occur (supplemental Fig. S6). The effect of KIF on the association of EDEMs with downstream ERAD machinery was examined further. In cells co-expressing E2 and EDEMs, the interaction of SEL1L with EDEM1 and EDEM3 was significantly reduced in the presence of KIF ($p < 0.05$) (Fig. 5*C*). Consistent with these results, KIF abrogated the EDEM1- and EDEM3-mediated ubiquitylation of HCV E2 protein (Fig. 5*D*). This inhibitory effect of KIF on the SEL1L-EDEM interaction was also observed in HuH-7 cells (supplemental Fig. S7). These results suggest that KIF stabilizes HCV glycoproteins by interfering with the SEL1L-EDEM interaction and thus leads to an increase in virus production.

Role of ERAD in the Life Cycle of JEV—This study demonstrates involvement of the ERAD pathway in HCV production. However, the role of this pathway in the production of other
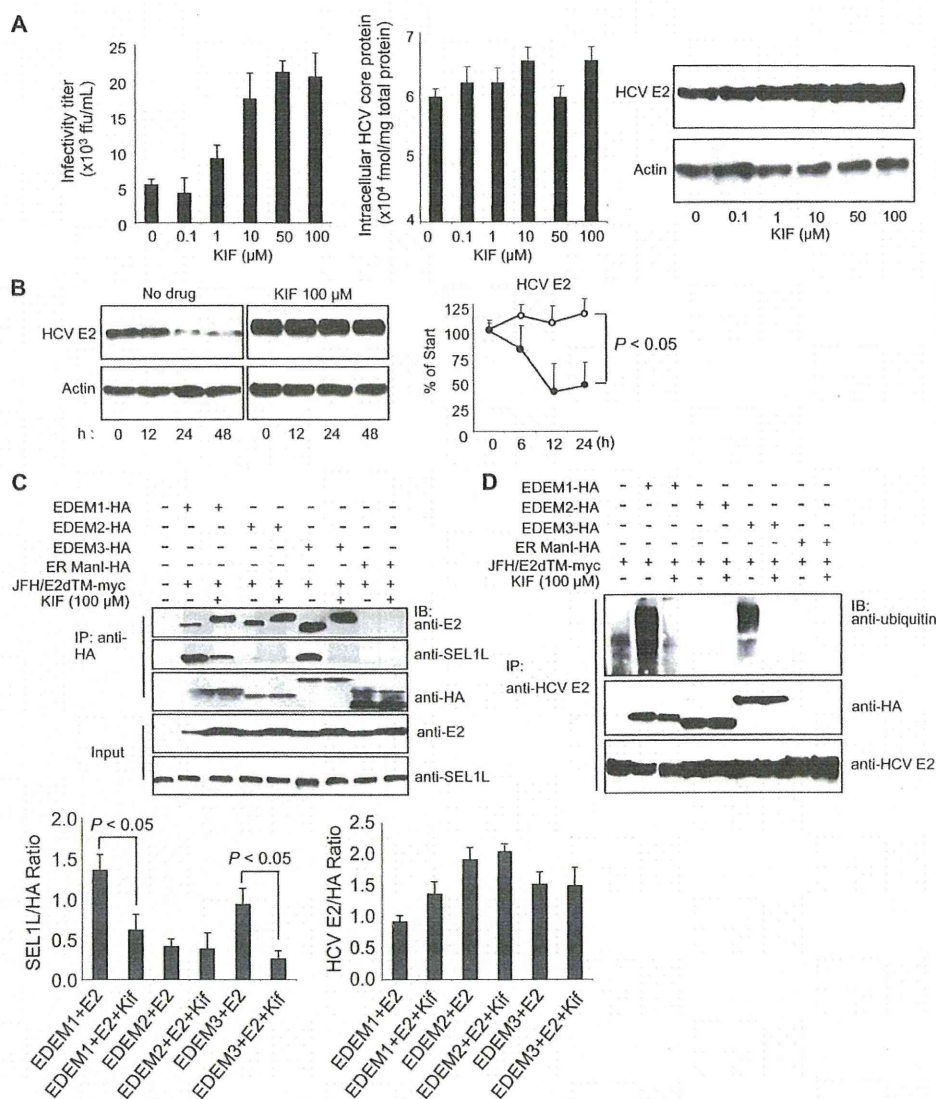
– 365 –

FIGURE 5. **Effect of KIF on HCV production and stability of E2.** *A*, extracellular HCV titer, intracellular HCV core protein expression, and steady-state level of HCV E2 in HuH-7 cells treated with different concentrations of KIF. *B*, CHX-based HCV protein stability assay of HCV E2 protein in KIF-treated cells as described in Fig. 3*E*. E2 protein levels normalized to actin levels are shown in the *graph* on the *right*. The *open* and *filled circles* indicate KIF-treated and nontreated cells, respectively. The mean ± S.D. (*error bars*) of two independent experiments are shown. *C*, binding of EDEMs and ER ManI with HCV E2 and SEL1L in 293T cells in the absence or presence of KIF. 293T cells were seeded in 6-well plates at a density of 3×10^5 cells/well. After overnight incubation, the cells were co-transfected with plasmids carrying HCV E2-myc (1 μg) and EDEM1-HA, EDEM2-HA, EDEM3-HA, or ER ManI-HA proteins (1 μg each). After 6 h, the culture medium was replaced with fresh or KIF-containing medium (100 μM). Forty-eight hours later, the cells were harvested and immunoprecipitated (*IP*) with anti-HA antibodies, after which Western blotting (*IB*) was performed with the indicated antibodies. Specific signals were quantified by densitometry, and the ratio between HCV E2 and HA (*right graph*) and between SEL1L and HA (*left graph*) in the same *lanes* is plotted on the graphs. The mean ± S.D. of three independent experiments are shown. *D*, EDEM protein-mediated ubiquitylation of HCV E2 protein in 293T cells in the absence or presence of KIF. The experimental procedure was the same as that described in Fig. 5*C*, except that immunoprecipitation was performed with anti-HCV E2 antibodies.

viruses is still unknown. To this end, we examined its role in the life cycle of JEV, another member of the Flaviviridae family. In contrast to HCV, KIF treatment had little effect on JEV production in infected cells (Fig. 6*A*) or the steady-state level of viral E glycoprotein (Fig. 6*B*). Interaction of EDEMs with JEV E was analyzed further. Neither EDEMs nor ER ManI was found to interact with JEV E in cells (Fig. 6*C*), indicating no significant role of the ERAD pathway in the JEV life cycle. Altogether, these results strongly suggest that the ERAD pathway is involved in the quality control of glycoproteins of specific viruses, possible through an interaction with EDEM(s), and subsequent regulation of virus production.

DISCUSSION

Accumulating evidence points to a role of the ERAD pathway in the pathogenesis of different genetic and degenerative diseases. However, the involvement of ERAD in the life cycle of viruses and infectious diseases remains poorly understood. Until recently, an experimental HCV cell culture infection system has been lacking such that studies evaluating the effect of HCV infection on the ERAD pathway were performed by either using HCV subgenomic replicons which lack structural proteins or by ectopic expression of one or multiple structural proteins (21, 22). However, this problem was solved by identifica-
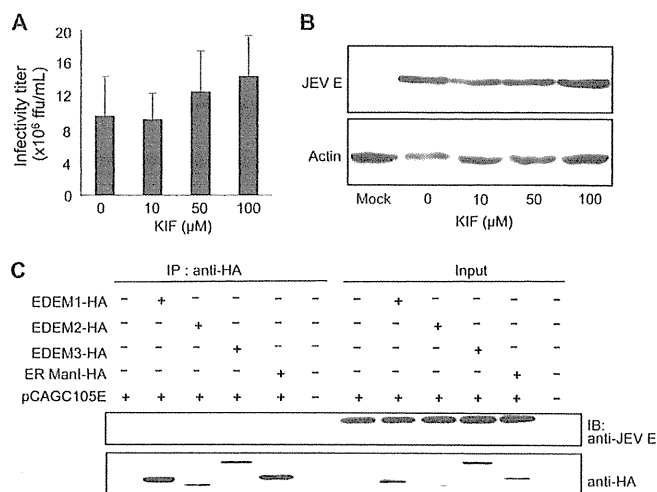
FIGURE 6. **Binding of JEV envelope glycoprotein with EDEMs and effect of KIF on JEV production.** *A*, JEV production in HuH-7 cells treated with KIF. The mean ± S.D. (*error bars*) of three independent experiments are shown. *B*, effect of KIF on the steady-state level of JEV envelope protein. *C*, binding of EDEMs with the JEV envelope.

tion of an HCV clone, JFH-1, capable of replicating and assembling infectious virus particles in cultured hepatocytes (15). In the present study, we used JFH-1 to examine the effect of HCV infection on activation of the ERAD pathway and its role in the virus life cycle. Our results show that the ERAD pathway is activated in HCV-infected cells, as evidenced by the maturation of XBP1 mRNA to its active form and up-regulation of EDEM1 (Fig. 1, *A–D*). Knocking down IRE1 reversed the induction of EDEM1, indicating that HCV infection-induced activation of the ERAD pathway is mediated through IRE1 (Fig. 1*F*). Loss- and gain-of-function analyses indicated that EDEM1 and EDEM3, particularly EDEM1, are involved in the post-translational control of HCV glycoproteins by which viral production is down-regulated (Figs. 3, *D* and *E*, and 4*A*). Our results suggest that EDEM1 and EDEM3 play a role in delivery of viral glycoproteins to the SEL1L-containing ubiquitin-ligase complex. It has recently been reported that coronavirus infection causes an accumulation of EDEM1 in membrane vesicles which are sites of viral replication, but that EDEM1 is not required for coronavirus replication (23). To our knowledge, the present study is the first to demonstrate regulation of the viral life cycle by ERAD machinery through interaction of EDEMs with viral glycoproteins.

We propose that the mechanisms described here are important during the early stages of establishing persistent HCV infection. ER stress caused by high levels of HCV infection during the acute phase presumably results in activation of the ERAD pathway. Induced EDEMs enhance the degradation of HCV envelope proteins, thereby reducing virus production. Maintenance of moderately low levels of HCV in the infected liver may contribute to the persistence of HCV infection, often associated with a lengthy asymptomatic phase that can last for decades. A range of viruses, including flaviviruses such as JEV, dengue virus, and West Nile virus, have been reported to induce XBP1 mRNA splicing triggered by ER stress (2, 3, 24). However, we demonstrate here that, in contrast to HCV, the envelope protein of JEV, which causes acute encephalitis, is not recog-

nized by EDEMs, and the ERAD pathway does not control JEV production.

N-Linked glycoproteins displaying the glycan precursor Glc1Man9GlcNAc2 bind ER chaperones, such as calnexin or calreticulin, which facilitates protein folding. Removal of the terminal Glc from glycans disrupts this interaction with chaperones leading to Man trimming and delivery to ERAD machinery. A glucosyltransferase can transfer the terminal Man-linked Glc back to glycans, thereby allowing the "calnexin cycle" to continue until the glycoproteins are properly folded (for review, see Ref. 25). During this cycle, the decision of when to abandon additional folding attempts for immature polypeptides and to direct them instead toward the degradation pathway appears to be a crucial element of protein quality control. The basis by which this occurs, however, is not fully understood. Here, we demonstrate that stabilization of HCV envelope proteins and increased virus production occurs with KIF treatment (Fig. 5, *A* and *B*) and with gene silencing of either EDEM1 or EDEM3 (Figs. 3, *D* and *E*, and 4*A*). It is generally accepted that ERAD functions to eliminate proteins that are unable to adopt their native structure after translocation into the ER. From our results, however, one could argue that, during the HCV life cycle, at least a fraction of the competently folded viral glycoprotein intermediates may be released from the calnexin cycle before maturation and thereby be recognized as ERAD substrates. As suggested previously, the processes of protein folding and ERAD compete to some extent for newly synthesized polypeptides (26, 27). Under conditions in which high concentrations of ERAD-related factors are found in the ER due to induction of ER stress by viral infection, activated ERAD machinery may efficiently capture protein intermediates with folding/refolding capacity and cause premature termination of chaperone-assisted protein folding.

EDEM1 has recently been found to bind SEL1L, which is involved in the translocation of ERAD substrates from the ER to the cytoplasm (20). Our results demonstrate efficient binding of EDEM1 and EDEM3 to SEL1L, whereas EDEM2 exhibits only residual binding. In agreement with these results, increased ubiquitylation of HCV E2 protein was observed in cells overexpressing EDEM1 and EDEM3, but not in cells overexpressing the EDEM2 ortholog (Fig. 3*B*). Furthermore, KIF inhibited the binding of EDEM1 and EDEM3 with SEL1L, thus abrogating the ubiquitylation and enhancing the stability of HCV E2 protein (Fig. 5, *B* and *D*). It has been reported that KIF inhibits the interaction between EDEM1 and SEL1L, thus stabilizing ERAD substrates (4). Therefore, our results confirm previous findings and show that, along with EDEM1, KIF inhibits the binding of SEL1L to EDEM3. Furthermore, we have been the first to show that HCV E2 is a virus-derived ERAD substrate that can be used to analyze the mechanisms of this pathway. Taken together, our results indicate that EDEM1 and EDEM3, but not EDEM2, might be involved in targeting ERAD substrates to the translocation machinery, which may partly explain the different roles of the three EDEMs in HCV production. Although both EDEM1 and EDEM3 bind SEL1L and HCV envelope proteins, EDEM1 appears to have a larger role in regulation of HCV production than EDEM3. This is supported further by the finding that enhanced ubiquitylation of HCV E2 occurs in the presence

- 367 -

of EDEM1 overexpression (Figs. 3*B* and 5*D*). In EDEM3-knockdown cells, EDEM1 may take over the function of delivering ERAD substrates to the translocation machinery. We also speculate that EDEM1 may function as a helper for EDEM3. This is supported by the observation that EDEM1 and EDEM3 synergistically increase HCV production when knocked down together (data not shown). HCV glycoproteins are a suitable means by which to investigate differences and redundancies pertaining to the role of EDEMs in the ERAD pathway.

HCV-infected and TM-treated cells demonstrated the greatest activation of EDEM1 transcript production among EDEMs (Fig. 1, *C* and *D*, and supplemental Fig. S1). Although it is known that XBP1 binds to specific ER stress-responsive *cis*-acting elements to induce EDEMs (28, 29), the exact mechanism of transcriptional regulation is not fully understood. It will be interesting to examine regulatory mechanism(s) specific to individual EDEM homologs in an ER stress-dependent or -independent manner.

These findings highlight the crucial role of the ERAD pathway in the HCV life cycle. Further studies are needed to clarify the details of this complex pathway. The data generated in this work, however, further contribute to our understanding of the mechanisms that govern the maturation and fate of viral glycoproteins in the ER.

REFERENCES

1. Vembar, S. S., and Brodsky, J. L. (2008) *Nat. Rev. Mol. Cell Biol.* **9**, 944–957
2. Yu, C. Y., Hsu, Y. W., Liao, C. L., and Lin, Y. L. (2006) *J. Virol.* **80**, 11868–11880
3. Barry, G., Fragkoudis, R., Ferguson, M. C., Lulla, A., Merits, A., Kohl, A., and Fazakerley, J. K. (2010) *J. Virol.* **84**, 7369–7377
4. Isler, J. A., Skalet, A. H., and Alwine, J. C. (2005) *J. Virol.* **79**, 6890–6899
5. Helenius, A., and Aebi, M. (2004) *Annu. Rev. Biochem.* **73**, 1019–1049
6. Mast, S. W., Diekman, K., Karaveg, K., Davis, A., Sifers, R. N., and Moremen, K. W. (2005) *Glycobiology* **15**, 421–436
7. Hirao, K., Natsuka, Y., Tamura, T., Wada, I., Morito, D., Natsuka, S., Romero, P., Sleno, B., Tremblay, L. O., Herscovics, A., Nagata, K., and Hosokawa, N. (2006) *J. Biol. Chem.* **281**, 9650–9658
8. Bartenschlager, R., and Lohmann, V. (2000) *J. Gen. Virol.* **81**, 1631–1648
9. Reed, K. E., and Rice, C. M. (2000) *Curr. Top. Microbiol. Immunol.* **242**, 55–84
10. Zhong, J., Gastaminza, P., Cheng, G., Kapadia, S., Kato, T., Burton, D. R., Wieland, S. F., Uprichard, S. L., Wakita, T., and Chisari, F. V. (2005) *Proc. Natl. Acad. Sci. U.S.A.* **102**, 9294–9299
11. Zhao, Z., Date, T., Li, Y., Kato, T., Miyamoto, M., Yasui, K., and Wakita, T. (2005) *J. Gen. Virol.* **86**, 2209–2220
12. Tani, H., Shiokawa, M., Kaname, Y., Kambara, H., Mori, Y., Abe, T., Moriishi, K., and Matsuura, Y. (2010) *J. Virol.* **84**, 2798–2807
13. Yoshida, H., Haze, K., Yanagi, H., Yura, T., and Mori, K. (1998) *J. Biol. Chem.* **273**, 33741–33749
14. Murakami, K., Kimura, T., Osaki, M., Ishii, K., Miyamura, T., Suzuki, T., Wakita, T., and Shoji, I. (2008) *J. Gen. Virol.* **89**, 1587–1592
15. Wakita, T., Pietschmann, T., Kato, T., Date, T., Miyamoto, M., Zhao, Z., Murthy, K., Habermann, A., Kräusslich, H. G., Mizokami, M., Bartenschlager, R., and Liang, T. J. (2005) *Nat. Med.* **11**, 791–796
16. Lim, C. K., Takasaki, T., Kotaki, A., and Kurane, I. (2008) *Virology* **374**, 60–70
17. Takeuchi, T., Katsume, A., Tanaka, T., Abe, A., Inoue, K., Tsukiyama-Kohara, K., Kawaguchi, R., Tanaka, S., and Kohara, M. (1999) *Gastroenterology* **116**, 636–642
18. Deng, L., Adachi, T., Kitayama, K., Bungyoku, Y., Kitazawa, S., Ishido, S., Shoji, I., and Hotta, H. (2008) *J. Virol.* **82**, 10375–10385
19. Masaki, T., Suzuki, R., Saeed, M., Mori, K., Matsuda, M., Aizaki, H., Ishii, K., Maki, N., Miyamura, T., Matsuura, Y., Wakita, T., and Suzuki, T. (2010) *J. Virol.* **84**, 5824–5835
20. Cormier, J. H., Tamura, T., Sunryd, J. C., and Hebert, D. N. (2009) *Mol. Cell* **34**, 627–633
21. Tardif, K. D., Mori, K., Kaufman, R. J., and Siddiqui, A. (2004) *J. Biol. Chem.* **279**, 17158–17164
22. Chan, S. W., and Egan, P. A. (2005) *FASEB J.* **19**, 1510–1512
23. Reggiori, F., Monastyrska, I., Verheije, M. H., Calì, T., Ulasli, M., Bianchi, S., Bernasconi, R., de Haan, C. A., and Molinari, M. (2010) *Cell Host Microbe* **7**, 500–508
24. Medigeshi, G. R., Lancaster, A. M., Hirsch, A. J., Briese, T., Lipkin, W. I., Defilippis, V., Früh, K., Mason, P. W., Nikolich-Zugich, J., and Nelson, J. A. (2007) *J. Virol.* **81**, 10849–10860
25. Molinari, M. (2007) *Nat. Chem. Biol.* **3**, 313–320
26. Eriksson, K. K., Vago, R., Calanca, V., Galli, C., Paganetti, P., and Molinari, M. (2004) *J. Biol. Chem.* **279**, 44600–44605
27. Wu, Y., Swulius, M. T., Moremen, K. W., and Sifers, R. N. (2003) *Proc. Natl. Acad. Sci. U.S.A.* **100**, 8229–8234
28. Olivari, S., Galli, C., Alanen, H., Ruddock, L., and Molinari, M. (2005) *J. Biol. Chem.* **280**, 2424–2428
29. Yoshida, H., Matsui, T., Hosokawa, N., Kaufman, R. J., Nagata, K., and Mori, K. (2003) *Dev. Cell* **4**, 265–271

– 368 –

Development of recombinant hepatitis C virus with NS5A from strains of genotypes 1 and 2

Yuka Okamoto [a,b], Takahiro Masaki [a], Asako Murayama [a], Tsubasa Munakata [c], Akio Nomoto [d], Shingo Nakamoto [e], Osamu Yokosuka [e], Haruo Watanabe [b,f], Takaji Wakita [a], Takanobu Kato [a,*]

[a] Department of Virology II, National Institute of Infectious Diseases, Shinjuku-ku, Tokyo 162-8640, Japan
[b] Department of Pathology, Immunology, and Microbiology, Graduate School of Medicine, The University of Tokyo, Bunkyo-ku, Tokyo 113-0033, Japan
[c] The Tokyo Metropolitan Institute of Medical Science, Setagaya-ku, Tokyo 156-8506, Japan
[d] Institute of Microbial Chemistry, Shinagawa-ku, Tokyo 141-0021, Japan
[e] Department of Medicine and Clinical Oncology, Graduate School of Medicine, Chiba University, Chiba 260-0856, Japan
[f] National Institute of Infectious Diseases, Shinjuku-ku, Tokyo 162-8640, Japan

ARTICLE INFO

ABSTRACT

Nonstructural protein 5A (NS5A) of hepatitis C virus (HCV) plays multiple and diverse roles in the viral lifecycle, and is currently recognized as a novel target for anti-viral therapy. To establish an HCV cell culture system with NS5A of various strains, recombinant viruses were generated by replacing NS5A of strain JFH-1 with those of strains of genotypes 1 (H77; 1a and Con1; 1b) and 2 (J6CF; 2a and MA; 2b). All these recombinant viruses were capable of replication and infectious virus production. The replacement of JFH-1 NS5A with those of genotype 1 strains resulted in similar or slightly reduced virus production, whereas replacement with those of genotype 2 strains enhanced virus production as compared with JFH-1 wild-type. A single cycle virus production assay with a CD81-negative cell line revealed that the efficient virus production elicited by replacement with genotype 2 strains depended on enhanced viral assembly, and that substitutions in the C-terminus of NS5A were responsible for this phenotype. Pulse-chase assays revealed that these substitutions in the C-terminus of NS5A were possibly associated with accelerated cleavage kinetics at the NS5A–NS5B site. Using this cell culture system with NS5A-substituted recombinant viruses, the anti-viral effects of an NS5A inhibitor were then examined. A 300- to 1000-fold difference in susceptibility to the inhibitor was found between strains of genotypes 1 and 2. This system will facilitate not only a better understanding of strain-specific roles of NS5A in the HCV lifecycle, but also enable the evaluation of genotype and strain dependency of NS5A inhibitors.

© 2011 Elsevier Inc. All rights reserved.

1. Introduction

Approximately 3% of the world's population is persistently infected with hepatitis C virus (HCV) and at increased risk of fatal chronic liver diseases such as decompensated liver cirrhosis and hepatocellular carcinoma. HCV have significant diversity in their genome and are grouped into six major genotypes. Among these genotypes, genotypes 1 and 2 are distributed worldwide and are predominant in Japan. The genotype is an important viral factor to predict the outcome of interferon (IFN)-based therapy. Because the efficacy of current therapy with pegylated IFN and ribavirin is insufficient, there is great interest in the development of novel HCV-specific inhibitors. The development of an HCV cell culture system with strain JFH-1 has enabled the study of the viral lifecycle and research into anti-viral compounds [1]. However, the available strains used in the HCV cell culture system are still limited to JFH-1 (genotype 2a) and H77S (genotype 1a) [2]. Thus, JFH-1 based recombinant viruses harboring specific regions of other strains would be useful to assess the genotype or strain-specific sensitivity to novel anti-HCV compounds.

Although NS5A is an essential and involved in HCV RNA replication and virus assembly [3,4], it has been reported to be tolerable for trans-complementation in replication-defective mutants due to critical mutations in NS5A [5]. We hypothesized that the NS5A of strain JFH-1 could be replaced with those of other strains. In the present study, we developed a cell culture system with JFH-1 based intra- and inter-genotypic recombinant HCV harboring NS5A of strains H77 (genotype 1a) [6], Con1 (genotype 1b) [7], J6CF (genotype 2a) [8], and MA (genotype 2b) [9]. Through the use of these recombinant viruses, we evaluated the effects of NS5A replacement on the HCV lifecycle and susceptibility to the NS5A inhibitor BMS-790052.

* Corresponding author. Address: Department of Virology II, National Institute of Infectious Diseases, 1-23-1 Toyama, Shinjuku-ku, Tokyo 162-8640, Japan. Fax: +81 3 5285 1161.
E-mail address: takato@nih.go.jp (T. Kato).

2. Materials and methods

2.1. Cell culture

The human hepatoma cell line, HuH-7, and derivative cell lines, Huh7.5.1 [10] and Huh7-25 [11], were cultured in complete growth medium as described previously [1,11].

2.2. Plasmid construction

Plasmids containing the full-genome of HCV strain JFH-1 (pJFH1) and of a replication defective mutant (pJFH1/GND) have been described previously [1]. The construction of the NS5A replaced recombinant viruses and subgenomic reporter replicons was described in Supplementary materials.

2.3. In vitro RNA synthesis and RNA transfection

In vitro synthesis of HCV RNA and RNA transfection were performed as described elsewhere [1].

2.4. Quantification of HCV core protein, luciferase activity, and extra- and intra-cellular infectivity

Quantification of these values was described in Supplementary materials.

2.5. Inhibition of HCV production by a specific NS5A inhibitor

Huh7.5.1 cells (3×10^6) were electroporated with 3 μg of synthetic HCV RNA, suspended in 15 mL complete growth medium, and seeded into 24-well plates. At 4 h after electroporation, the culture medium was replaced with medium containing 0.1% dimethyl sulfoxide (DMSO) with or without various concentrations of the specific NS5A inhibitor BMS-790052 (provided from Bristol-Myers Squibb Company, Plainsboro, NJ) [12]. After 44 h incubation, cells were harvested and HCV core protein was quantified.

2.6. Statistical analysis

Unpaired 2-tailed t-test was performed to evaluate the significance of results, and $p < 0.05$ was considered significant.

3. Results

3.1. Development of recombinant HCV with NS5A of genotypes 1 and 2

To establish an HCV cell culture system with NS5A of various strains, we generated recombinant viruses by replacing NS5A of strain JFH-1 with those of genotypes 1 and 2 strains. By transfection of in vitro transcribed RNA, efficient production of HCV core protein was detected in JFH-1 wild-type (JFH1/wt) and other recombinant viruses, but not in the replication defective mutant JFH1/GND (Fig. 1A). When compared between JFH1/wt and other recombinant viruses, intracellular core protein levels were comparable at days 2 and 3 after transfection, while extracellular core protein levels were very different. The extracellular core protein level of JFH1/wt-transfected cells increased exponentially up to $23,515 \pm 1790$ fmol/L at day 3. Similar kinetics was observed in JFH1/5A-H77-transfected cells. However, the extracellular core protein level of JFH1/5A-Con1-transfected cells was approximately 2.5-fold lower than that of JFH1/wt at days 2 and 3. Interestingly, the extracellular core protein levels of intra-genotypic recombinant viruses, JFH1/5A-J6CF and 5A-MA, were 2.5- to 3.5-fold higher than that of JFH1/wt at days 2 and 3. To evaluate the effect of these

NS5A replacements on HCV replication, we used recombinant subgenomic reporter replicons, SGR-JFH1/RLuc/wt, 5A-H77, 5A-Con1, 5A-J6CF, and 5A-MA. The Renilla luciferase activities of these recombinant subgenomic replicons were comparable to that of SGR-JFH1/Rluc/wt, suggesting similar levels of replication efficiency (Fig. 1B).

To further assess whether NS5A replacement affected other steps of the viral lifecycle, we used a single cycle virus production assay with Huh7-25 cells, a HuH-7-derived cell line lacking CD81 expression on the cell surface [11]. This cell line can support replication and infectious virus production upon transfection of HCV genomic RNA, but cannot be reinfected by produced HCV, therefore allowing the observation of a single cycle of infectious viral production without the confounding effects of reinfection [13]. As shown in Fig. 1C, JFH1/wt yielded an extracellular infectivity titer of 1585 ± 436 FFU/well at day 2 after transfection. JFH1/5A-H77 and 5A-Con1 showed significantly lower titers, while JFH1/5A-J6CF and 5A-MA showed significantly higher intracellular infectivity titers compared to JFH1/wt ($p < 0.05$). These data were consistent with the extracellular core protein levels of JFH1/wt and recombinant viruses (Fig. 1A). A similar tendency was observed in the intracellular infectivity titers of JFH1/wt and recombinant viruses (Fig. 1C). To estimate the efficiency of viral particle assembly, we determined the intracellular specific infectivity by calculating the ratio of the intracellular infectivity titer over the intracellular HCV core protein level. The intracellular specific infectivities of JFH1/5A-H77 and 5A-Con1 were 2.5- and 8-fold lower than that of JFH1/wt, respectively, while JFH1/5A-J6CF and 5A-MA showed 12- and 4-fold higher infectivities compared to JFH1/wt, respectively, suggesting a low assembly efficiency of JFH1/5A-H77 and 5A-Con1, and a high assembly efficiency of JFH1/5A-J6CF and 5A-MA (Fig. 1D). Taken together, all recombinant viruses could replicate and yielded infectious virus. Intra-genotypic recombinant viruses, JFH1/5A-J6CF and 5A-MA, had a higher ability to produce infectious virus than JFH1/wt in cultured cells.

3.2. The C-terminus of NS5A is responsible for enhanced viral assembly

The efficient infectious virus production of intra-genotypic recombinant viruses was unexpected. This prompted us to search for causes of the enhancement. To analyze the enhanced virus assembly of JFH1/5A-J6CF and 5A-MA, we focused on the C-terminus of NS5A of these strains, because this region influence the cleavage between NS5A and NS5B, and the cleavage is reported to be involved in virus assembly [14]. We generated recombinant JFH-1 viruses harboring 10 amino acids of the C-terminus of NS5A of J6CF and MA (JFH1/5AcJ6 and 5AcMA, respectively), and investigated replication and infectious virus production. In these 10 amino acids of the C-terminus of NS5A, JFH1/5AcJ6 and 5AcMA contain 2 and 6 substitutions, respectively, as compared with JFH1/wt, and 2 of them, T2438S and T2439V, are common (Fig. 2A). As shown in Fig. 2B, the extracellular core protein level of JFH1/5AcJ6-transfected cells was higher than those of JFH1/wt- and 5A-J6CF-transfected cells at the examined time points. A similar tendency was observed between JFH1/5AcMA and JFH1/wt or 5A-MA (Fig. 2C). In contrast to the extracellular core protein levels, the intracellular core protein levels were comparable for all NS5A recombinants at the examined time points.

We next assessed the replication of recombinant subgenomic luciferase reporter replicons on the basis of JFH1/5AcJ6 and 5AcMA (Fig. 2D). JFH1/5AcJ6 and 5AcMA showed similar levels of replication to JFH1/wt at day 2 after transfection. To investigate the effects of substitutions at the C-terminus of NS5A on infectious viral particle assembly, we determined the extra- and intracellular infectivity with the single cycle virus production assay with Huh7-25 cells. As shown in Fig. 2E, extra- and intracellular infectivities of
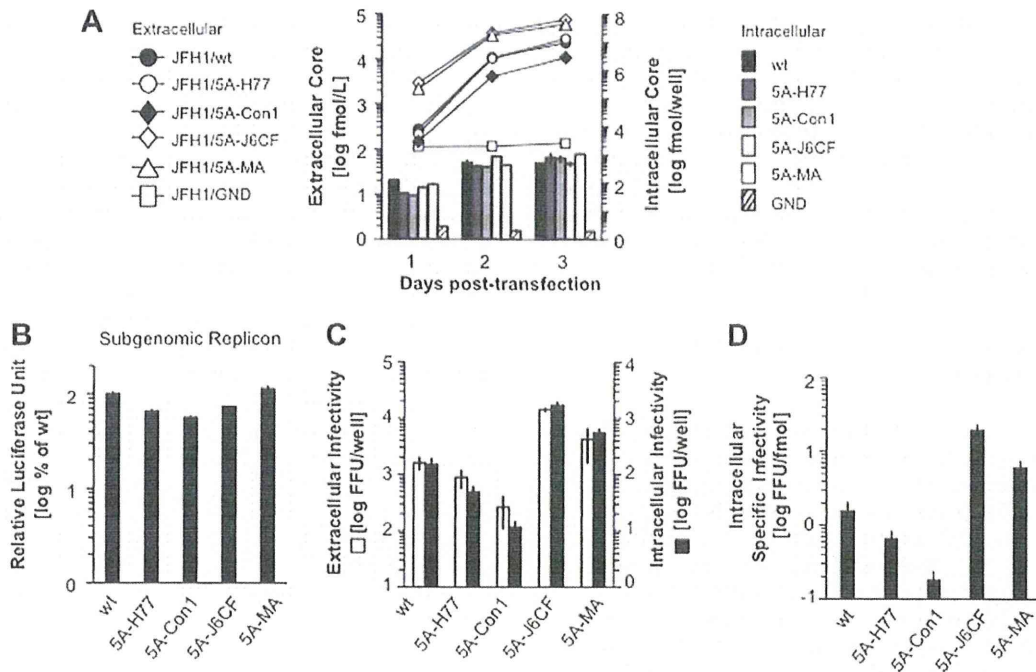
Fig. 1. Production and replication of recombinant viruses with NS5A of strains of genotypes 1 and 2. (A) Huh7.5.1 cells were transfected with in vitro synthesized RNA of JFH1/wt and indicated recombinants. The amount of extracellular (line graph) and intracellular (bar graph) HCV core protein was determined at the indicated time points. Assays were performed in triplicate, and means ± standard deviation are plotted. (B) Huh7.5.1 cells were transfected with subgenomic replicon RNA of JFH1/wt and indicated recombinants. Luciferase activity at day 2 was measured. Replication levels of JFH1/wt and indicated recombinants were calculated as fold increases at 4 h and are expressed as percentages of JFH1/wt. (C) Huh7-25 cells were transfected with RNA of JFH1/wt and recombinants. Forty-eight hours after transfection, extra- and intracellular infectivities were determined by inoculating into naïve Huh7.5.1 cells. (D) Intracellular specific infectivity of JFH1/wt and indicated recombinants.
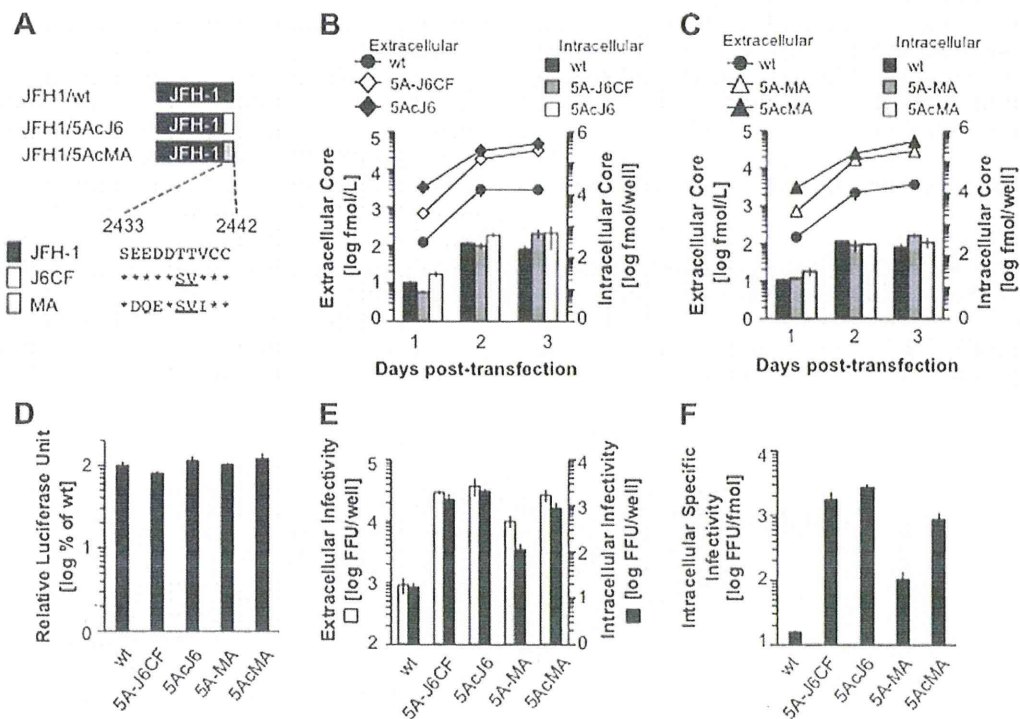

Fig. 2. C-terminal amino acids in NS5A were responsible for the enhanced virus production of recombinant viruses with NS5A of genotype 2 strains. (A) Alignment of C-terminal amino acids in NS5A of JFH-1, J6CF, and MA. Identical amino acids are indicated by asterisks. The indicated number represents the position of the amino acid in the entire polyprotein of JFH-1. (B) Huh7.5.1 cells were transfected with RNA of JFH1/wt, 5A-J6CF, and 5AcJ6. The amount of extracellular (line graph) and intracellular (bar graph) core proteins were quantified at the indicated time points. (C) Huh7.5.1 cells were transfected with RNA of JFH1/wt, 5A-MA, and 5AcMA. The amount of extracellular (line graph) and intracellular (bar graph) core proteins were quantified at the indicated time points. (D) Huh7.5.1 cells were transfected with subgenomic replicon RNA of JFH1/wt and indicated recombinants. Luciferase activity at day 2 was measured. Replication levels of JFH1/wt and indicated recombinants were calculated as the fold increase at 4 h and are expressed as percentages of JFH1/wt. (E) Huh7-25 cells were transfected with RNA of JFH1/wt and recombinant viruses. Forty-eight hours after transfection, extra- and intracellular infectivities were determined by inoculating into naïve Huh7.5.1 cells. (F) Intracellular specific infectivities of JFH1/wt and indicated recombinants.

JFH1/5AcJ6 and 5AcMA were approximately 20-fold higher than that of the JFH1/wt ($p < 0.05$), and were slightly higher than those of JFH1/5A-J6CF and 5A-MA. We also determined the specific intracellular infectivity of each recombinant virus to assess virus assembly (Fig. 2F). As with extra- and intracellular infectivities, the specific intracellular infectivities of JFH1/5AcJ6 and 5AcMA were more than 10-fold higher than that of the JFH1/wt ($p < 0.05$), and were slightly higher than those of JFH1/5A-J6CF and 5A-MA. These results suggest that these C-terminal amino acids of NS5A are responsible for enhanced assembly of intra-genotypic recombinant viruses JFH1/5A-J6CF and 5A-MA.

3.3. Amino acid substitutions at the C-terminus of NS5A accelerate cleavage kinetics between NS5A and NS5B

To investigate whether substitution of the C-terminus of NS5A affects the cleavage kinetics between NS5A and NS5B, we performed pulse-chase assays using a T7-based expression system. Immunoprecipitations were performed with an NS5B-specific antibody and immunocomplexes were analyzed on a 7.5% SDS–PAGE (Supplementary Fig. A). Fully processed NS5B and an uncleaved NS5A–NS5B precursor with a size of approximately 130 kDa could be detected for JFH1/wt and recombinant constructs JFH1/5AcJ6 and 5AcMA. In the case of JFH1/wt, the amount of uncleaved precursor was gradually decreased but still detectable at 4 h of the chase period. On the other hand, in the case of the recombinant constructs, JFH1/5AcJ6 and 5AcMA, the amounts of precursor were reduced more rapidly and were undetectable by 4 h of chase. To assess the kinetics of the cleavage, the percentages of uncleaved NS5A–NS5B precursor at the examined time points were plotted and analyzed using nonlinear regression (Supplementary Fig. B). Rapid cleavage kinetics was observed in JFH1/5AcJ6 and 5AcMA transfected cells as compared with JFH1/wt. These observations suggest that substitutions at the C-terminus of NS5A of these recombinant viruses are responsible for the accelerated cleavage kinetics between NS5A and NS5B, and might be associated with enhanced infectious viral particle assembly.

3.4. Susceptibility of recombinant HCV to the NS5A inhibitor BMS-790052

Using developed JFH-1 based inter- and intra-genotypic recombinant viruses, we assessed their susceptibility to the NS5A inhibitor BMS-790052 [12]. After transfection with synthesized HCV RNA, cells were treated with different concentrations of BMS-790052 for 2 days and intracellular HCV core protein levels were

determined. No cytopathic effects were observed at the concentrations used (data not shown). As shown in Fig. 3, the intracellular core protein levels of JFH1/wt and recombinant viruses were inhibited to different extents. Recombinant viruses with NS5A of genotype 1, JFH1/5A-H77 and 5A-Con1, showed higher susceptibility to BMS-790052 as compared with JFH1/wt, while JFH1/5A-J6CF and 5A-MA showed much lower susceptibility. To compare the susceptibilities, the effective concentrations required to inhibit 50% of intracellular core protein level (EC_{50}) were determined, because the intracellular core protein levels of these recombinant viruses were at almost the same level at day 2 after transfection (Fig. 1A). The EC_{50} of JFH1/wt and recombinant viruses with NS5A of genotype 1, JFH1/5A-H77 and 5A-Con1, were 6.4, 3.1, and 1.4 pM, respectively, and do not conflict with results using replicon systems reported previously [12]. In contrast, recombinant viruses with NS5A of genotype 2, JFH1/5A-J6CF and 5A-MA, were more resistant to BMS-790052, and EC_{50} values were 1.5 and >5 nM, respectively. Collectively, the anti-HCV effect of the specific NS5A inhibitor BMS-790052 showed strain and genotype dependency. In particular, the NS5A of genotype 2 strains, J6CF and MA, excepting JFH-1, showed 300- to 1000-fold lower susceptibility to BMS-790052 compared with the NS5A of genotype 1 strains, H77 and Con1.

4. Discussion

HCV NS5A is essential for replication and infectious virus production, similar to other nonstructural proteins possessing enzymatic activities, including NS3 (a serine protease) and NS5B (an RNA-dependent RNA polymerase). Currently, these nonstructural proteins are being targeted to establish anti-viral compounds to improve the outcome of therapy for chronic HCV infection, and several inhibitors for these proteins are entering into clinical trials. A great deal of interest has also been shown in the development of NS5A inhibitors, and one potent inhibitor, BMS-790052, has recently been described [12]. In this study, to assess strain and genotype dependent susceptibility for this inhibitor, we generated recombinant HCV with NS5A from strains other than JFH-1, because a limited number of strains are available in the HCV cell culture system. We replaced NS5A of JFH-1 with those of genotype 1 and 2 strains, and observed efficient replication and infectious virus production in cell culture.

The replication efficiencies of these NS5A recombinant viruses were almost the same, whereas virus production levels into the culture medium were very different from JFH1/wt (Fig. 1A and
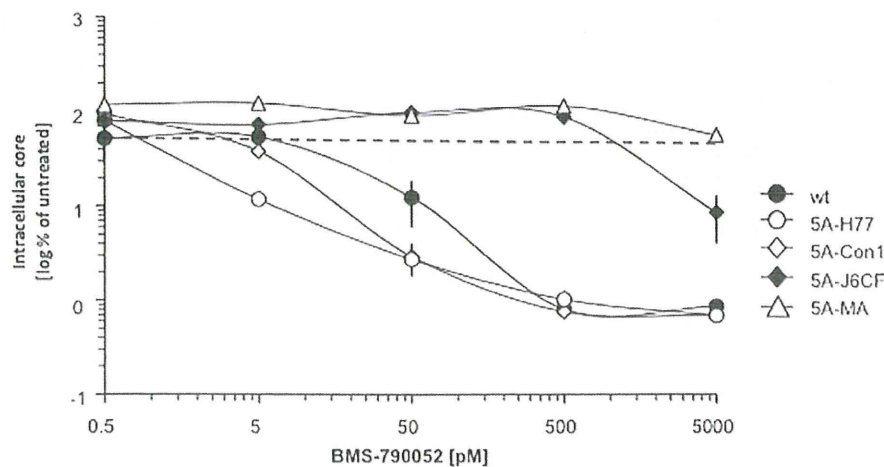

Fig. 3. Susceptibility of JFH1/wt and recombinant viruses to the NS5A inhibitor. Huh7.5.1 cells were transfected with RNA of JFH1/wt and recombinant viruses and treated with serially diluted BMS-790052 for 48 h. The amounts of intracellular HCV core protein were quantified and normalized against untreated control set to 100%.

Table 1
Amino acid substitutions in NS5A of strains used, and reported resistant mutations to BMS-790052.

AA[a]		Strains used in this study					Reported resistant mutations[b]			Ref.
Entire	NS5A	JFH1	H77	Con1	J6CF	MA	1a	1b	2a	
2004	28	F	M	L	F	L	T (683)	T (20)	–	[20]
2006	30	K	Q	R	K	K	E (24,933)	E (6)	–	[20]
							K (24,317)			
							H (1450)			
							R (1217)			
2007	31	L	L	L	M	M	M (350)	F (5)	M (170)	[12,20]
							V (3350)	M (3)		
								V (23)		
2008	32	P	P	P	P	P	L (233)	L (17)	–	[20]
2068	93	A	A	C	C	C	–	–	E (150)	[12]
2069	93	Y	Y	Y	Y	Y	C (1850)	H (19)	H (130–1400)	[12,20]
							H (5367)	N (28)		
							N (47,017)			

[a] AA, amino acid position which are according to entire polyprotein (Entire) and NS5A of JFH1.
[b] Fold resistance as compared with parental amino acid is indicated in parentheses.

B). Enhanced virus production was detected in recombinant viruses replaced with NS5A of genotype 2 strains, while reduced virus production was observed in recombinant viruses replaced with NS5A of genotype 1 strains (Fig. 1A). The single cycle virus production assay revealed that this enhanced virus production with NS5A of genotype 2 was due to efficient viral particle assembly (Fig. 1D). To analyze the mechanism of efficient virus assembly by NS5A of strains J6CF and MA, we focused on the cleavage between NS5A and NS5B. Several reports have shown that amino acids in the C-terminus of NS5A influence the cleavage [15,16]. Thus, we used recombinant JFH-1 viruses harboring amino acids of J6CF and MA in the C-terminus of JFH-1 NS5A, and assessed replication and infectious virus production. We found that both of these recombinant viruses, JFH1/5AcJ6 and 5AcMA, showed more enhanced virus assembly (Fig. 2F), and reasoned that the amino acid substitutions T2438S and T2439V were responsible for the enhanced infectious virus production. In pulse-chase assays for the cleavage of NS5A and NS5B, accelerated cleavage was observed in recombinant viruses JFH1/5AcJ6 and 5AcMA. Uncleaved NS5A–NS5B disappeared earlier in JFH1/5AcJ6- and 5AcMA-transfected cells than in JFH1/wt-transfected cells (Supplementary Fig. A). Taken together, the enhanced virus assembly observed with JFH1/5A-J6CF and 5A-MA depended on the C-terminal amino acid substitutions in NS5A, possibly through accelerated cleavage kinetics between NS5A and NS5B. The reason for the correlation between accelerated cleavage and enhanced virus assembly is still unknown. Accelerated cleavage may lead to an increased amount of mature NS5A used for virus assembly or affect the interaction with the core protein, which has been reported to be important for infectious virus assembly [17]. Another possibility is the interaction between the C-terminus of NS5A and some host factor(s) involved in virus particle assembly, such as apolipoprotein E [18]. Amino acid substitutions at this region may alter the potency of this interaction directly. A previous report has also shown that another mutation in this region, V2440L, is associated with delayed cleavage kinetics between NS5A and NS5B, but enhanced virus assembly [14]. Further investigation will be necessary to clarify this mechanism and to solve the discrepancy.

Using this cell culture system with NS5A recombinant viruses, we assessed strain and genotype dependent susceptibility to the novel NS5A inhibitor, BMS-790052. This potent inhibitor successfully inhibited replication of JFH1/wt and recombinant viruses with NS5A of genotype 1 strains (Fig. 3). However, it showed limited effectiveness on recombinant viruses with NS5A of genotype 2 strains. This high efficacy for genotype 1 strains makes sense because this inhibitor and its lead compound were identified using genotype 1a and 1b subgenomic replicons [19].

During preparation of this paper, another study was published describing an HCV cell culture system with NS5A-substituted recombinant viruses [20]. That study used a J6/JFH-1 chimeric virus that is known to have high virus production efficiency, but not natural viruses, and established nine recombinant viruses with NS5A from strains of eight different subtypes. They found that recombinant viruses with NS5A of strains of genotypes 1a, 1b, 4a, 5a, and 6a were sensitive, and strains of genotypes 2a and 3a were resistant to the NS5A inhibitor, data that are consistent with our own observations. In addition, we found that recombinant virus with NS5A of genotype 2b, which is the one of the predominant genotypes in Japan, was also resistant to the compound. Resistant mutations to BMS-790052 have been reported and are frequently observed in the N-terminus of NS5A, suggesting inhibition of membrane localization and dimerization of NS5A (Table 1) [12,20]. Among these reported mutations, one of the most potent, 2006E/K/H/R (amino acid position (AA) 30 in NS5A), is found in all strains but H77, and another potent resistant mutation, 2007F/M/V (AA 31 in NS5A), is also found in J6CF and MA. Thus, the lower susceptibilities of recombinant viruses JFH1/5A-J6CF and 5A-MA, as compared with JFH1/wt, might be due to the latter mutation. Based on an analysis of the database of submitted strains (Hepatitis Virus Database; http://s2as02.genes.nig.ac.jp/index.html), this resistant mutation, 2007M, is detected in 84.2% and 79.0% of genotype 2a and 2b strains, respectively, whereas it is observed in only 0.2% of genotype 1a and 3.8% of genotype 1b strains [20,21]. From these observations, most of genotype 2a and 2b strains may be resistant to BMS-790052, although these are known to be sensitive to interferon [22].

In conclusion, we established JFH-1 based recombinant viruses by replacement of NS5A with those from strains of genotypes 1 and 2. All the generated recombinant viruses could replicate and produce infectious viruses in cell culture, and were useful to assess the genotype and strain dependency to a novel NS5A inhibitor. The strategy of using recombinant virus will facilitate not only a better understanding of the strain-specific roles of NS5A in the HCV lifecycle, but also aid in developing and testing specific inhibitors against NS5A from different genotypes and strains.

Appendix A. Supplementary data

Supplementary data associated with this article can be found, in the online version, at doi:10.1016/j.bbrc.2011.05.144.

References

[1] T. Wakita, T. Pietschmann, T. Kato, T. Date, M. Miyamoto, Z. Zhao, K. Murthy, A. Habermann, H.G. Krausslich, M. Mizokami, R. Bartenschlager, T.J. Liang, Production of infectious hepatitis C virus in tissue culture from a cloned viral genome, Nat. Med. 11 (2005) 791–796.

[2] M. Yi, R.A. Villanueva, D.L. Thomas, T. Wakita, S.M. Lemon, Production of infectious genotype 1a hepatitis C virus (Hutchinson strain) in cultured human hepatoma cells, Proc. Natl. Acad. Sci. USA 103 (2006) 2310–2315.

[3] M.J. Evans, C.M. Rice, S.P. Goff, Phosphorylation of hepatitis C virus nonstructural protein 5A modulates its protein interactions and viral RNA replication, Proc. Natl. Acad. Sci. USA 101 (2004) 13038–13043.

[4] N. Appel, M. Zayas, S. Miller, J. Krijnse-Locker, T. Schaller, P. Friebe, S. Kallis, U. Engel, R. Bartenschlager, Essential role of domain III of nonstructural protein 5A for hepatitis C virus infectious particle assembly, PLoS Pathog. 4 (2008) e1000035.

[5] N. Appel, U. Herian, R. Bartenschlager, Efficient rescue of hepatitis C virus RNA replication by trans-complementation with nonstructural protein 5A, J. Virol. 79 (2005) 896–909.

[6] M. Yanagi, R.H. Purcell, S.U. Emerson, J. Bukh, Transcripts from a single full-length cDNA clone of hepatitis C virus are infectious when directly transfected into the liver of a chimpanzee, Proc. Natl. Acad. Sci. USA 94 (1997) 8738–8743.

[7] V. Lohmann, F. Korner, J. Koch, U. Herian, L. Theilmann, R. Bartenschlager, Replication of subgenomic hepatitis C virus RNAs in a hepatoma cell line, Science 285 (1999) 110–113.

[8] M. Yanagi, R.H. Purcell, S.U. Emerson, J. Bukh, Hepatitis C virus: an infectious molecular clone of a second major genotype (2a) and lack of viability of intertypic 1a and 2a chimeras, Virology 262 (1999) 250–263.

[9] K. Murakami, M. Abe, T. Kageyama, N. Kamoshita, A. Nomoto, Down-regulation of translation driven by hepatitis C virus internal ribosomal entry site by the 3' untranslated region of RNA, Arch. Virol. 146 (2001) 729–741.

[10] J. Zhong, P. Gastaminza, G. Cheng, S. Kapadia, T. Kato, D.R. Burton, S.F. Wieland, S.L. Uprichard, T. Wakita, F.V. Chisari, Robust hepatitis C virus infection in vitro, Proc. Natl. Acad. Sci. USA 102 (2005) 9294–9299.

[11] D. Akazawa, T. Date, K. Morikawa, A. Murayama, M. Miyamoto, M. Kaga, H. Barth, T.F. Baumert, J. Dubuisson, T. Wakita, CD81 expression is important for the permissiveness of Huh7 cell clones for heterogeneous hepatitis C virus infection, J. Virol. 81 (2007) 5036–5045.

[12] M. Gao, R.E. Nettles, M. Belema, L.B. Snyder, V.N. Nguyen, R.A. Fridell, M.H. Serrano-Wu, D.R. Langley, J.H. Sun, D.R. O'Boyle 2nd, J.A. Lemm, C. Wang, J.O. Knipe, C. Chien, R.J. Colonno, D.M. Grasela, N.A. Meanwell, L.G. Hamann, Chemical genetics strategy identifies an HCV NS5A inhibitor with a potent clinical effect, Nature 465 (2010) 96–100.

[13] T. Kato, Y. Choi, G. Elmowalid, R.K. Sapp, H. Barth, A. Furusaka, S. Mishiro, T. Wakita, K. Krawczynski, T.J. Liang, Hepatitis C virus JFH-1 strain infection in chimpanzees is associated with low pathogenicity and emergence of an adaptive mutation, Hepatology 48 (2008) 732–740.

[14] A. Kaul, S. Stauffer, C. Berger, T. Pertel, J. Schmitt, S. Kallis, M. Zayas, V. Lohmann, J. Luban, R. Bartenschlager, Essential role of cyclophilin A for hepatitis C virus replication and virus production and possible link to polyprotein cleavage kinetics, PLoS Pathog. 5 (2009) e1000546.

[15] R. Bartenschlager, L. Ahlborn-Laake, K. Yasargil, J. Mous, H. Jacobsen, Substrate determinants for cleavage in cis and in trans by the hepatitis C virus NS3 proteinase, J. Virol. 69 (1995) 198–205.

[16] A. Urbani, E. Bianchi, F. Narjes, A. Tramontano, R. De Francesco, C. Steinkuhler, A. Pessi, Substrate specificity of the hepatitis C virus serine protease NS3, J. Biol. Chem. 272 (1997) 9204–9209.

[17] T. Masaki, R. Suzuki, K. Murakami, H. Aizaki, K. Ishii, A. Murayama, T. Date, Y. Matsuura, T. Miyamura, T. Wakita, T. Suzuki, Interaction of hepatitis C virus nonstructural protein 5A with core protein is critical for the production of infectious virus particles, J. Virol. 82 (2008) 7964–7976.

[18] W. Cun, J. Jiang, G. Luo, The C-terminal alpha-helix domain of apolipoprotein E is required for interaction with nonstructural protein 5A and assembly of hepatitis C virus, J. Virol. 84 (2010) 11532–11541.

[19] J.A. Lemm, D. O'Boyle 2nd, M. Liu, P.T. Nower, R. Colonno, M.S. Deshpande, L.B. Snyder, S.W. Martin, D.R. St Laurent, M.H. Serrano-Wu, J.L. Romine, N.A. Meanwell, M. Gao, Identification of hepatitis C virus NS5A inhibitors, J. Virol. 84 (2010) 482–491.

[20] T.K. Scheel, J.M. Gottwein, L.S. Mikkelsen, T.B. Jensen, J. Bukh, Recombinant HCV variants with NS5A from genotypes 1–7 have different sensitivities to an NS5A inhibitor but not interferon-alpha, Gastroenterology 140 (2011) 1032–1042.

[21] R.A. Fridell, D. Qiu, C. Wang, L. Valera, M. Gao, Resistance analysis of the hepatitis C virus NS5A inhibitor BMS-790052 in an in vitro replicon system, Antimicrob. Agents Chemother. 54 (2010) 3641–3650.

[22] K. Yoshioka, S. Kakumu, T. Wakita, T. Ishikawa, Y. Itoh, M. Takayanagi, Y. Higashi, M. Shibata, T. Morishima, Detection of hepatitis C virus by polymerase chain reaction and response to interferon-alpha therapy: relationship to genotypes of hepatitis C virus, Hepatology 16 (1992) 293–299.

Short Communication

Structural requirements of virion-associated cholesterol for infectivity, buoyant density and apolipoprotein association of hepatitis C virus

Mami Yamamoto,[1,2] Hideki Aizaki,[1] Masayoshi Fukasawa,[3]
Tohru Teraoka,[2] Tatsuo Miyamura,[1] Takaji Wakita[1] and Tetsuro Suzuki[1,4]

Correspondence

Tetsuro Suzuki

tesuzuki@hama-med.ac.jp

[1]Department of Virology II, National Institute of Infectious Diseases, Toyama 1-23-1, Shinjuku-ku, Tokyo 162-8640, Japan

[2]United Graduate School of Agricultural Science, Tokyo University of Agriculture and Technology, Saiwai-cho 3-5-8, Fuchu, Tokyo 183-8509, Japan

[3]Department of Biochemistry and Cell Biology, National Institute of Infectious Diseases, Toyama 1-23-1, Shinjuku-ku, Tokyo 162-8640, Japan

[4]Department of Infectious Diseases, Hamamatsu University School of Medicine, Handayama 1-20-1, Higashi-ku, Hamamatsu 431-3192, Japan

Our earlier study has demonstrated that hepatitis C virus (HCV)-associated cholesterol plays a key role in virus infectivity. In this study, the structural requirement of sterols for infectivity, buoyant density and apolipoprotein association of HCV was investigated further. We removed cholesterol from virions with methyl β-cyclodextrin, followed by replenishment with 10 exogenous cholesterol analogues. Among the sterols tested, dihydrocholesterol and coprostanol maintained the buoyant density of HCV and its infectivity, and 7-dehydrocholesterol restored the physical appearance of HCV, but suppressed its infectivity. Other sterol variants with a 3β-hydroxyl group or with an aliphatic side chain did not restore density or infectivity. We also provide evidence that virion-associated cholesterol contributes to the interaction between HCV particles and apolipoprotein E. The molecular basis for the effects of different sterols on HCV infectivity is discussed.

Hepatitis C virus (HCV) is a major cause of liver diseases, and is an enveloped, plus-strand RNA virus of the genus *Hepacivirus* of the family *Flaviviridae*. The mature HCV virion is considered to consist of a nucleocapsid, an outer envelope composed of the viral E1 and E2 proteins and a lipid membrane. Production and infection of several enveloped viruses, such as human immunodeficiency virus type 1 (HIV-1), hepatitis B virus and varicella-zoster virus (Bremer *et al.*, 2009; Campbell *et al.*, 2001; Graham *et al.*, 2003; Hambleton *et al.*, 2007), are dependent on cholesterol associated with virions. However, except for HIV-1 (Campbell *et al.*, 2002, 2004), there is limited information about the effects of replacing cholesterol with sterol analogues on the virus life cycle. We demonstrated the higher cholesterol content of HCV particles compared with host-cell membranes, and that HCV-associated cholesterol plays a key role in virion maturation and infectivity (Aizaki *et al.*, 2008). Recently, by using mass spectrometry, Merz *et al.* (2011) identified cholesteryl esters, cholesterol,

phosphatidylcholine and sphingomyelin as major lipids of purified HCV particles.

To investigate further the effect of the structural requirement for cholesterol on the infectivity, buoyant density and apolipoprotein association of HCV, depletion of virion-associated cholesterol and substitution of endogenous cholesterol with structural analogues (Fig. 1a) was used in this study. HCVcc (HCV grown in cell culture) of the JFH-1 isolate (Wakita *et al.*, 2005), prepared as described previously (Aizaki *et al.*, 2008), was treated with 1 mM methyl β-cyclodextrin (B-CD), which extracts cholesterol from biological membranes, for 1 h at 37 °C. The cholesterol-depleted virus was then incubated with exogenous cholesterol or cholesterol analogues at various concentrations for 1 h. After removal of B-CD and free sterols by centrifugation at 38 000 r.p.m. (178 000 *g*) for 2.5 h, the treated particles were used to infect Huh7 cells, kindly provided by Dr Francis V. Chisari (The Scripps Research Institute, La Jolla, CA, USA), and their infectivity was determined by quantifying the viral core protein in cells using an enzyme immunoassay (Ortho-Clinical Diagnostics) at 3 days post-infection (p.i.). Virus infectivity, which fell to <20% after B-CD treatment, was

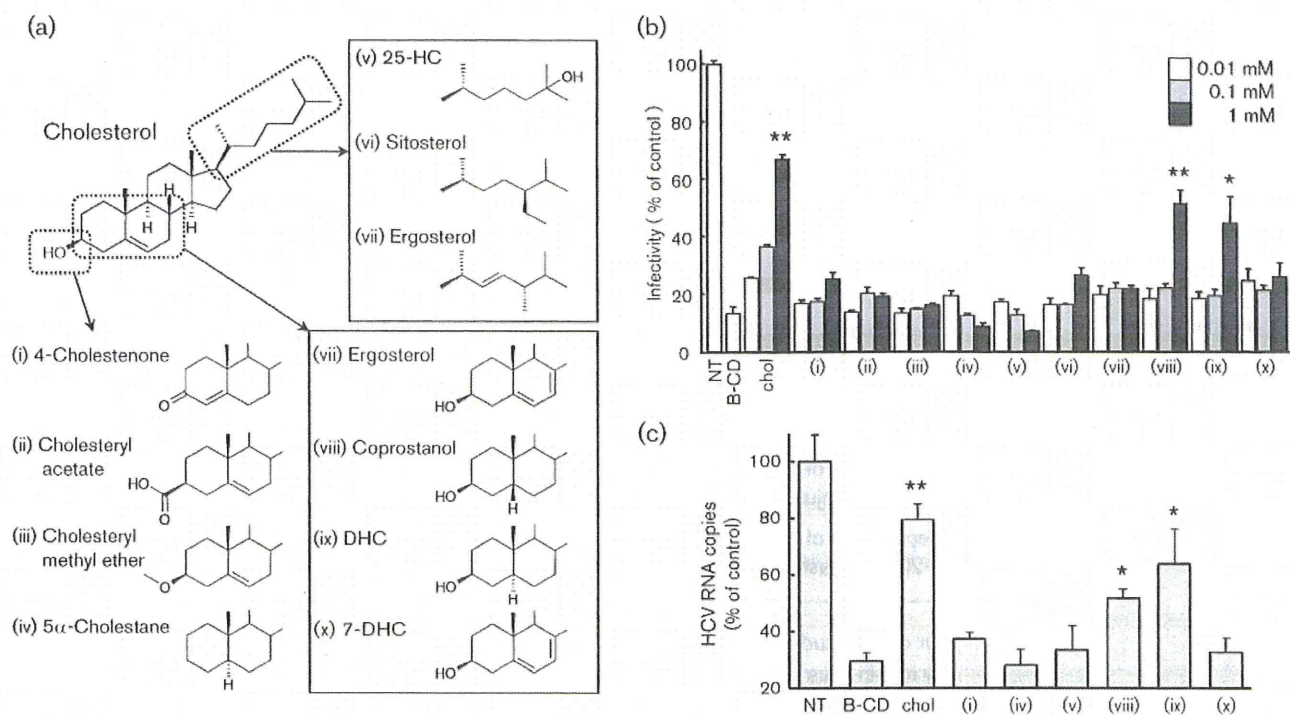**Fig. 1.** Role of virion-associated cholesterol analogues in virus infection. (a) Structures of sterols used in this study. Variations in the 3β-hydroxyl group (lower left), aliphatic side chain (upper right) or ring structure (lower right) of cholesterol are shown. (i–x) Compounds studied in (b) and (c). (b) Effect of replenishment with sterols on HCV infectivity. Intracellular HCV core levels were determined at 72 h p.i. as the indicator of infectivity, which is represented as a percentage of the untreated HCVcc level (NT). (c) Effects of virion-associated sterols on virus internalization. HCV RNA copies in cells after virus internalization were quantified and are shown as percentages of the untreated HCVcc level (NT). (b, c) Means + SD of four samples are shown. *$P<0.05$; **$P<0.01$, compared with B-CD-treated virus (unpaired Student's t-test). Data are representative of at least two experiments.

recovered by addition of cholesterol at 0.01–1 mM in a dose-dependent manner (Fig. 1b). Among the cholesterol analogues tested, variants with a 3β-hydroxyl group (4-cholestenone, cholesteryl acetate, cholesteryl methyl ether and 5α-cholestane) or variants with an aliphatic side chain [25-hydroxycholesterol (25-HC), sitosterol and ergosterol] exhibited no or little effect on the recovery of infectivity of B-CD-treated HCV (Fig. 1b, lanes i–vii). In contrast, addition of variants in the structure of the sterol rings [coprostanol or dihydrocholesterol (DHC)] at 1 mM restored infectivity to around 50 % compared with non-treated virus control (Fig. 1b, lanes viii and ix). Other variants in the ring structure [7-dehydrocholesterol (7-DHC) and ergosterol, which is also a variant with an aliphatic side chain as indicated above] did not show any increase in the infectivity of B-CD-treated virus (Fig. 1b, lanes x and vii).

We demonstrated previously that HCV-associated cholesterol plays an important role in the internalization step of the virus, but not in cell attachment during virus entry (Aizaki *et al.*, 2008). The effect of virion-associated cholesterol analogues on virus attachment to cells and

following internalization was determined. HCVcc, treated with B-CD with or without subsequent replenishment with sterols, was incubated with Huh7-25-CD81 cells, which stably express CD81 (Akazawa *et al.*, 2007), for 1 h at 4 °C. As an internalization assay, the incubation temperature was shifted to 37 °C post-binding procedure and maintained for 2 h. The cells were then treated with 0.25 % trypsin for 10 min at 37 °C, by which >90 % of HCV bound to the cell surface was removed (data not shown; Aizaki *et al.*, 2008). Internalized HCV was quantified by measuring the viral RNA in cell lysates by real-time RT-PCR (Takeuchi *et al.*, 1999). B-CD treatment or supplementation with sterols of B-CD-treated HCV had little or no effect on virus attachment to the cell surface (data not shown). Regarding virus internalization (Fig. 1c), treatment of HCVcc with 1 mM B-CD resulted in approximately 70 % reduction of viral RNA. The reduced level of the internalized HCV recovered markedly to approximately 80 % of the untreated HCVcc level by replenishment with 1 mM cholesterol. In agreement with the results shown in Fig. 1(b), addition of coprostanol or DHC to the B-CD-treated virus caused a significant recovery of virus internalization, suggesting that coprostanol and DHC associated with the

virion have the ability to play a role in HCV internalization into cells, in a manner comparable to cholesterol (Fig. 1c, lanes viii and ix). No or only a little recovery of virus internalization was observed by loading with other cholesterol analogues, such as 4-cholestenone, 5α-cholestane, 25-HC or 7-DHC (Fig. 1c, lanes i, iv, v and x).

To monitor the effect of cholesterol analogues on the physical characteristics of HCV, we next investigated buoyant-density profiles by using sucrose density-gradient centrifugation, in which untreated, B-CD-treated and sterol-replenished HCVcc were concentrated and layered onto continuous 10–60 % (w/v) sucrose density gradients, followed by centrifugation at 35 000 r.p.m. (151 000 g) for 14 h. Fractions were collected and analysed for the core protein. Fig. 2 shows that the virus density became higher after treatment with B-CD and that cholesterol-replenished virus shifted the density of B-CD-treated HCV to the non-treated level. Consistent with the result shown in Fig. 1(b), no effect on restoration of the buoyant densities of HCV was observed using variants with modifications in either the 3β-hydroxyl group (4-cholestenone, cholesteryl acetate and 5α-cholestane) or the aliphatic side chain (25-HC and sitosterol). In contrast, variants in the sterol ring structure (coprostanol, DHC and 7-DHC) had an ability to recover the density of B-CD-treated virus to that of non-treated virus.

Incorporation efficiency of the sterols into the cholesterol-depleted HCVcc was further determined by gas chromatography with flame ionization detection (see Supplementary Table S1, available in JGV Online). Under the experimental

conditions used, exogenously supplied cholesterol after B-CD treatment was able to restore cholesterol content in HCVcc almost to initial levels. When 4-cholestenone, cholesteryl acetate, 25-HC, DHC or 7-DHC was added to B-CD-treated HCVcc, virion-associated sterol levels were 146, 157, 68, 96 or 73 %, respectively, of that of the non-treated control. The proportion of cholesterol analogues to the total sterols incorporated was ≥30 % when 4-cholestenone, cholesteryl acetate, DHC or 7-DHC was used; however, the proportion in the case of 25-HC was only 3 %. It may be that the hydrophilic modification of the aliphatic side chain leads to poor association with HCVcc.

Collectively, exogenous variants with the 3β-hydroxyl group, such as 4-cholestenone and cholesteryl acetate, can be incorporated into B-CD-treated HCVcc, but resulted in no recovery of virus infectivity, indicating the importance of the 3β-hydroxyl group of cholesterol associated with the virus envelope in HCV infectivity. In contrast, two variants with modification in their sterol ring structures, coprostanol and DHC, have the ability to substitute for cholesterol. However, 7-DHC, another variant within the sterol ring, is incorporated readily into the depleted virion and restores the virus density, HCV replenished with 7-DHC is not infectious. These facts suggest that reduced forms of the sterol ring (coprostanol and DHC) in virion-associated cholesterol can be permitted for maintaining virus infectivity. However, a molecule with an additional double bond in the ring structure (7-DHC) seems to fail to exhibit infectivity, presumably because the change reduces structural flexibility in the
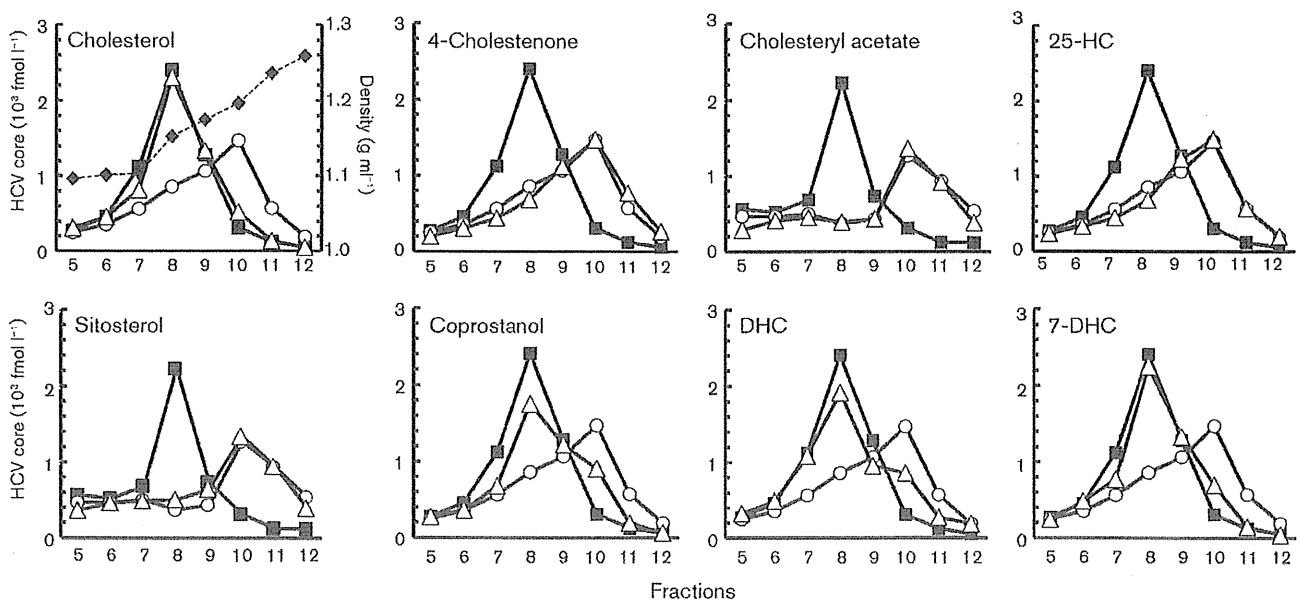

Fig. 2. Sucrose density-gradient profiles of lipid-modified HCV. Core protein concentration in each fraction of untreated HCVcc (■), B-CD-treated HCVcc (○) or HCVcc replenished with sterols (△) was determined. Corresponding densities of fractions are shown as a dashed line (◆).

sterol molecule and consequently in the virion structure. Coprostanol and DHC are *cis* and *trans* isomers, which are often known to have different physical properties. However, based on their molecular models, these two sterols, as well as cholesterol, possibly have similar spatial arrangements of the aliphatic side chain, the hydroxyl group and four-ring region because of their structural flexibility. In contrast, the spatial arrangement of 7-DHC does not seem comparable to that of cholesterol. Campbell *et al.* (2004) reported that replacement of HIV-1-associated cholesterol with raft-inhibiting sterols, including coprostanol, suppresses HIV-1 infectivity, whereas replacement with raft-promoting analogues such as DHC and 7-DHC (Megha *et al.*, 2006; Wang *et al.*, 2004; Xu & London, 2000; Xu *et al.*, 2001) maintains infectivity, demonstrating the importance of the raft-promoting properties of virion-associated cholesterol in HIV-1 infectivity (Campbell *et al.*, 2004). It is therefore likely that HCV-associated cholesterol is involved, at least in part, in virus infectivity via a molecular basis independent of lipid-raft formation.

The density of blood-circulating HCV is heterogeneous, ranging approximately from <1.06 to 1.25 g ml^{-1}, and it is proposed that low-density virus is associated with very-low-density lipoprotein (VLDL) and/or low-density lipoprotein (LDL) (André *et al.*, 2002; Thomssen *et al.*, 1993). It has recently been demonstrated that the pathway for VLDL assembly plays a role in assembly and maturation of infectious HCVcc (Icard *et al.*, 2009). HCVcc with low density, which is presumably associated with VLDL or VLDL-like lipoproteins, was found to possess higher infectivity than that with high density (Lindenbach *et al.*, 2006). This study, as well as our earlier work, indicated that removal of cholesterol from HCVcc by B-CD increased the buoyant density of the virus and reduced its infectivity. Thus, one may hypothesize that the virion-associated cholesterol plays a role in the formation of a complex with lipoproteins or apolipoproteins. To address this, the interaction between apolipoproteins and HCVcc with or without B-CD treatment was investigated by co-immunoprecipitation (Co-IP kit; Thermo Scientific). Virus samples were subjected separately to AminoLink Plus coupling resin, which was conjugated with a monoclonal antibody (mAb) against apolipoprotein E (ApoE) or apolipoprotein B (ApoB), and incubated at 4 °C for 4 h. After washing, total RNAs were extracted from the resulting resin beads by using TRIzol reagent (Invitrogen), followed by quantification of HCV RNA as described above (Takeuchi *et al.*, 1999). As indicated in Fig. 3(a), only a fraction of HCVcc was precipitated with an anti-ApoB mAb. In contrast, an anti-ApoE mAb was able to coprecipitate a considerable amount of the virus. It is of interest that B-CD-treated HCVcc hardly reacted with the mAb; however, the cholesterol-replenished virus was found to recover its reactivity, suggesting a role for virion-associated cholesterol in the formation of the HCV–lipoprotein/apolipoprotein complex. The results obtained are consistent with findings indicating that HCVcc can be captured with anti-ApoE antibodies, but capture with anti-ApoB antibodies is inefficient (Chang *et al.*, 2007; Hishiki *et al.*, 2010; Huang *et al.*, 2007; Jiang & Luo, 2009; Merz *et al.*, 2011; Nielsen *et al.*, 2006; Owen *et al.*, 2009), as well as with a recent model of structures of infectious HCV, in which HCVcc looks like ApoE-positive and primarily ApoB-negative lipoproteins (Bartenschlager *et al.*, 2011). We further tested the ApoE distribution in the density-gradient fractions of HCVcc samples (see Supplementary Fig. S1, available in JGV Online). With or without cholesterol depletion, ApoE was detected at a wide range of concentrations: 1.04 g ml^{-1} (fraction 1) to 1.17 g ml^{-1} (fraction 9). However, its level in the fractions at 1.10 g ml^{-1} (fraction 5) to approximately 1.17 g ml^{-1} was moderately decreased in the case of B-CD-treated virus.
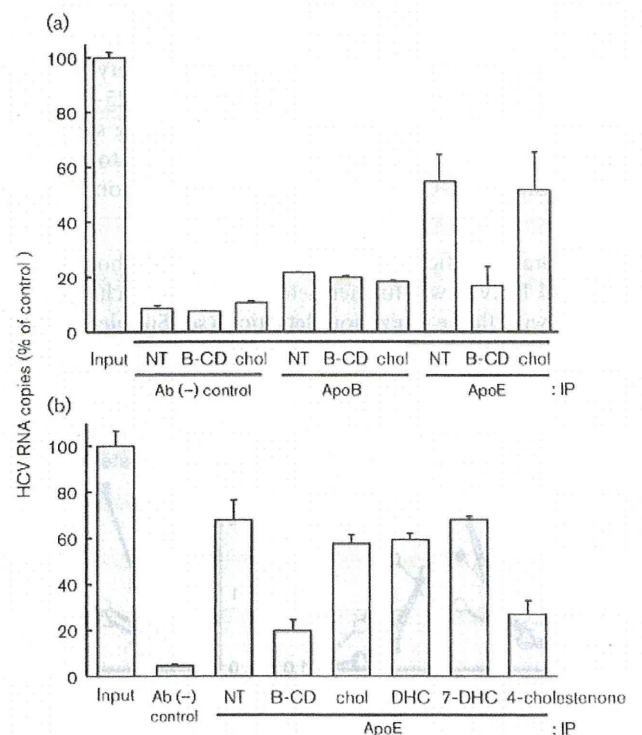

Fig. 3. Effect of virion-associated sterols on HCV–apolipoprotein interaction. (a) HCVcc samples with no treatment (NT), B-CD-treated (B-CD) or replenished with cholesterol (chol) were incubated with an amine-reactive resin coupling either an anti-ApoB mAb (ApoB) or an anti-ApoE mAb (ApoE). Control resin that is composed of the same material as above, but is not activated, was used as a negative control [Ab (−) control]. (b) B-CD-treated HCVcc was incubated with cholesterol (chol), DHC, 7-DHC or 4-cholestenone, followed by immunoprecipitation with the resin coupling with anti-ApoE mAb. (a, b) HCV RNAs in the immunoprecipitates were quantified and are indicated as percentages of the amount of input HCVcc RNA. Means+SD of three samples are shown. Data are representative of three experiments.

Whether cholesterol analogues could have a comparable role in HCV association with lipoprotein was examined further (Fig. 3b). Addition of DHC or 7-DHC, but not 4-cholestenone, to B-CD-treated HCVcc resulted in the recovery of coprecipitation of the virus with anti-ApoE. The results are correlated with the effect of sterols on the restoration of the buoyant densities of lipid-modified HCVcc (Fig. 2), suggesting that virion-associated cholesterol variants with modification in the sterol rings, but not in either the 3β-hydroxyl group or the aliphatic side chain, may tolerate the interaction between HCV and ApoE-positive lipoprotein.

Given that 7-DHC restored the association of HCV with ApoE and virion buoyant density, but did not restore infectivity, cholesterol and/or its analogues might affect the ability of virion membranes to fuse with the cell, independent of ApoE association. As cholesterol is an important mediator of membrane fluidity, one may hypothesize that HCV-associated cholesterol is involved in infectivity through modulation of the membrane fluidity. It has been reported that, in patients with Smith–Lemli–Opitz syndrome, a disorder of the cholesterol-synthesis pathway, cholesterol content decreases and 7-DHC increases in the cell membranes, leading to alteration of phospholipid packing in the membrane and abnormal membrane fluidity (Tulenko et al., 2006).

It is now accepted that maturation and release of infectious HCV coincide with the pathway for producing VLDLs, which export cholesterol and triglyceride from hepatocytes. This study revealed roles for the structural basis of virion-associated cholesterol in the infectivity, buoyant density and apolipoprotein association of HCV. Although it was shown that HCV virions in infected patients, so-called lipo–viro particles, exhibited certain biochemical properties such as containing ApoB, ApoC and ApoE (Diaz et al., 2006; Bartenschlager et al., 2011), our studies provide useful information and the basis for future investigations toward a deeper understanding of the biogenesis pathway of infectious HCV particles.

Acknowledgements

References

Aizaki, H., Morikawa, K., Fukasawa, M., Hara, H., Inoue, Y., Tani, H., Saito, K., Nishijima, M., Hanada, K. & other authors (2008). Critical role of virion-associated cholesterol and sphingolipid in hepatitis C virus infection. *J Virol* 82, 5715–5724.

Akazawa, D., Date, T., Morikawa, K., Murayama, A., Miyamoto, M., Kaga, M., Barth, H., Baumert, T. F., Dubuisson, J. & Wakita, T. (2007). CD81 expression is important for the permissiveness of Huh7 cell clones for heterogeneous hepatitis C virus infection. *J Virol* 81, 5036–5045.

André, P., Komurian-Pradel, F., Deforges, S., Perret, M., Berland, J. L., Sodoyer, M., Pol, S., Bréchot, C., Paranhos-Baccalà, G. & Lotteau, V. (2002). Characterization of low- and very-low-density hepatitis C virus RNA-containing particles. *J Virol* 76, 6919–6928.

Bartenschlager, R., Penin, F., Lohmann, V. & André, P. (2011). Assembly of infectious hepatitis C virus particles. *Trends Microbiol* 19, 95–103.

Bremer, C. M., Bung, C., Kott, N., Hardt, M. & Glebe, D. (2009). Hepatitis B virus infection is dependent on cholesterol in the viral envelope. *Cell Microbiol* 11, 249–260.

Campbell, S. M., Crowe, S. M. & Mak, J. (2001). Lipid rafts and HIV-1: from viral entry to assembly of progeny virions. *J Clin Virol* 22, 217–227.

Campbell, S. M., Crowe, S. M. & Mak, J. (2002). Virion-associated cholesterol is critical for the maintenance of HIV-1 structure and infectivity. *AIDS* 16, 2253–2261.

Campbell, S., Gaus, K., Bittman, R., Jessup, W., Crowe, S. & Mak, J. (2004). The raft-promoting property of virion-associated cholesterol, but not the presence of virion-associated Brij 98 rafts, is a determinant of human immunodeficiency virus type 1 infectivity. *J Virol* 78, 10556–10565.

Chang, K. S., Jiang, J., Cai, Z. & Luo, G. (2007). Human apolipoprotein E is required for infectivity and production of hepatitis C virus in cell culture. *J Virol* 81, 13783–13793.

Diaz, O., Delers, F., Maynard, M., Demignot, S., Zoulim, F., Chambaz, J., Trépo, C., Lotteau, V. & André, P. (2006). Preferential association of hepatitis C virus with apolipoprotein B48-containing lipoproteins. *J Gen Virol* 87, 2983–2991.

Graham, D. R., Chertova, E., Hilburn, J. M., Arthur, L. O. & Hildreth, J. E. (2003). Cholesterol depletion of human immunodeficiency virus type 1 and simian immunodeficiency virus with β-cyclodextrin inactivates and permeabilizes the virions: evidence for virion-associated lipid rafts. *J Virol* 77, 8237–8248.

Hambleton, S., Steinberg, S. P., Gershon, M. D. & Gershon, A. A. (2007). Cholesterol dependence of varicella-zoster virion entry into target cells. *J Virol* 81, 7548–7558.

Hishiki, T., Shimizu, Y., Tobita, R., Sugiyama, K., Ogawa, K., Funami, K., Ohsaki, Y., Fujimoto, T., Takaku, H. & other authors (2010). Infectivity of hepatitis C virus is influenced by association with apolipoprotein E isoforms. *J Virol* 84, 12048–12057.

Huang, H., Sun, F., Owen, D. M., Li, W., Chen, Y., Gale, M., Jr & Ye, J. (2007). Hepatitis C virus production by human hepatocytes dependent on assembly and secretion of very low-density lipoproteins. *Proc Natl Acad Sci U S A* 104, 5848–5853.

Icard, V., Diaz, O., Scholtes, C., Perrin-Cocon, L., Ramière, C., Bartenschlager, R., Penin, F., Lotteau, V. & André, P. (2009). Secretion of hepatitis C virus envelope glycoproteins depends on assembly of apolipoprotein B positive lipoproteins. *PLoS One* 4, e4233.

Jiang, J. & Luo, G. (2009). Apolipoprotein E but not B is required for the formation of infectious hepatitis C virus particles. *J Virol* 83, 12680–12691.

Lindenbach, B. D., Meuleman, P., Ploss, A., Vanwolleghem, T., Syder, A. J., McKeating, J. A., Lanford, R. E., Feinstone, S. M., Major, M. E. & other authors (2006). Cell culture-grown hepatitis C virus is infectious *in vivo* and can be recultured *in vitro*. *Proc Natl Acad Sci U S A* 103, 3805–3809.

Megha, Bakht, O. & London, E. (2006). Cholesterol precursors stabilize ordinary and ceramide-rich ordered lipid domains (lipid

rafts) to different degrees. Implications for the Bloch hypothesis and sterol biosynthesis disorders. *J Biol Chem* 281, 21903–21913.

Merz, A., Long, G., Hiet, M. S., Brügger, B., Chlanda, P., Andre, P., Wieland, F., Krijnse-Locker, J. & Bartenschlager, R. (2011). Biochemical and morphological properties of hepatitis C virus particles and determination of their lipidome. *J Biol Chem* 286, 3018–3032.

Nielsen, S. U., Bassendine, M. F., Burt, A. D., Martin, C., Pumeechockchai, W. & Toms, G. L. (2006). Association between hepatitis C virus and very-low-density lipoprotein (VLDL)/LDL analyzed in iodixanol density gradients. *J Virol* 80, 2418–2428.

Owen, D. M., Huang, H., Ye, J. & Gale, M., Jr (2009). Apolipoprotein E on hepatitis C virion facilitates infection through interaction with low-density lipoprotein receptor. *Virology* 394, 99–108.

Takeuchi, T., Katsume, A., Tanaka, T., Abe, A., Inoue, K., Tsukiyama-Kohara, K., Kawaguchi, R., Tanaka, S. & Kohara, M. (1999). Real-time detection system for quantification of hepatitis C virus genome. *Gastroenterology* 116, 636–642.

Thomssen, R., Bonk, S. & Thiele, A. (1993). Density heterogeneities of hepatitis C virus in human sera due to the binding of beta-lipoproteins and immunoglobulins. *Med Microbiol Immunol (Berl)* 182, 329–334.

Tulenko, T. N., Boeze-Battaglia, K., Mason, R. P., Tint, G. S., Steiner, R. D., Connor, W. E. & Labelle, E. F. (2006). A membrane defect in the pathogenesis of the Smith–Lemli–Opitz syndrome. *J Lipid Res* 47, 134–143.

Wakita, T., Pietschmann, T., Kato, T., Date, T., Miyamoto, M., Zhao, Z., Murthy, K., Habermann, A., Kräusslich, H. G. & other authors (2005). Production of infectious hepatitis C virus in tissue culture from a cloned viral genome. *Nat Med* 11, 791–796.

Wang, J., Megha & London, E. (2004). Relationship between sterol/steroid structure and participation in ordered lipid domains (lipid rafts): implications for lipid raft structure and function. *Biochemistry* 43, 1010–1018.

Xu, X. & London, E. (2000). The effect of sterol structure on membrane lipid domains reveals how cholesterol can induce lipid domain formation. *Biochemistry* 39, 843–849.

Xu, X., Bittman, R., Duportail, G., Heissler, D., Vilcheze, C. & London, E. (2001). Effect of the structure of natural sterols and sphingolipids on the formation of ordered sphingolipid/sterol domains (rafts). Comparison of cholesterol to plant, fungal, and disease-associated sterols and comparison of sphingomyelin, cerebrosides, and ceramide. *J Biol Chem* 276, 33540–33546.

– 380 –